

Chemistry of *C*-Trimethylsilyl-Substituted Heterocarboranes. 26. Further Investigation of Oxidative Cage Closure, Cage Fusion, and Cage Isomerizations: Synthetic, Structural, and Bonding Studies on “Carbons Adjacent” and “Carbons Apart” Tetracarba-*nido*-dodecaborane(12) Derivatives[†]

Narayan S. Hosmane,^{*,‡,§} Thomas J. Colacot,[§] Hongming Zhang,[§] Jimin Yang,[§]
John A. Maguire,^{*,§} Ying Wang,[§] Maria B. Ezhova,[§] Andreas Franken,[§]
Temesgen Demissie,^{§,||} Kai-Juan Lu,[§] Dunming Zhu,[§] Julie L. C. Thomas,[§]
Jess D. Collins,[§] Thomas G. Gray,[§] Suneil N. Hosmane,[§] and
William N. Lipscomb^{*,||}

*Department of Chemistry, Southern Methodist University, Dallas, Texas 75275, and
Department of Biophysics, Harvard University, Cambridge, Massachusetts 02138*

Received July 16, 1998

A number of tetracarbon carboranes of the general form $(\text{SiMe}_3)_2(\text{R})_2\text{C}_4\text{B}_8\text{H}_8$ ($\text{R} = \text{SiMe}_3$ (**III** and **IV**) Me (**XIII** and **XIV**), n -Bu (**VII**, **XI**, and **XII**), t -Bu (**VIII**)) were synthesized by the reactions of the corresponding mono- or dianions of *nido*-2-(SiMe_3)-3-(R)-2,3- $\text{C}_2\text{B}_4\text{H}_6$ with NiCl_2 in n -hexane. The *nido*-carboranes where $\text{R} = n$ -Bu (**I**), t -Bu (**II**) are newly reported and were obtained from the reaction of $\text{Me}_3\text{SiC}\equiv\text{CR}$ with B_5H_9 . The tetracarbon compounds were minor products of the reactions, with yields ranging from 13% for **VIII** to 37% for **XI**; the major products were the corresponding *closo*-1-(SiMe_3)-2-(R)-1,2- $\text{C}_2\text{B}_4\text{H}_4$ compounds, which were obtained in yields from 69% ($\text{R} = t$ -Bu (**VI**)) to 32% ($\text{R} = \text{SiMe}_3$). The *closo*-carboranes where $\text{R} = n$ -Bu (**V**), t -Bu (**VI**) could be converted to the more stable *closo*-1-(SiMe_3)-6-(R)-1,6- $\text{C}_2\text{B}_4\text{H}_4$ ($\text{R} = n$ -Bu (**IX**), t -Bu (**X**)) by heating to 250–255 °C for 4–5 h; this agrees with previous studies on the compounds where $\text{R} = \text{SiMe}_3$, Me . To aid in cage structure determination, a monobrominated, tetracarbon carborane, **XV**, was prepared from the reaction of **VII** with Br_2 in n -hexane, in 46% yield. All compounds were characterized by their ^1H , ^{11}B , and ^{13}C NMR spectra and elemental analyses and by the following: **I**–**XIV** by their IR spectra; **III**, **IV**, **VII**–**X**, **XIII**, and **XIV** by mass spectrometry; and **III**, **IV**, **XI**, **XII**, and **XV** by single-crystal X-ray crystallography. Depending on the structures of the C_4B_8 cages, the compounds could be classified as having “carbons apart” structures, in which all cage carbons were separated by at least one boron atom (**III**, **IV**, **VII**, **VIII**, **XIV**, and **XV**), or “carbons adjacent” structures, in which the carbons were localized on the same side of the clusters (**XI**–**XIII**). Compound **III** is unique in that its structure is that of a distorted cuboctahedron, while **IV** and **XV** are *nido*-carboranes having a C_3B_3 face that surmounts a B_5 ring and an apical cage carbon atom; none of the rings are planar, and the apical carbon is unequally bonded to the B_5 ring atoms. Similarities in their NMR spectra indicate that **VII** and **VIII** have structures similar to **IV** and **XV**. Two types of “carbons adjacent” cages were identified: one typified by **XI**, in which the four cage carbons are bonded contiguously, and a more open cage, in which the bond between the middle two carbons is broken (**XII**). All of the C_4B_8 compounds were found to have nonrigid stereochemistries; both the ^{11}B and ^{13}C NMR spectra of the “carbons apart” compounds consisted of single resonance peaks, indicating rapid atom equilibration on the NMR time scale. The “carbons adjacent” compounds showed ^{11}B NMR spectra of six resonance peaks; each had a different chemical shift and peak-area ratio pattern. The ^{11}B NMR spectra of the “carbons apart” isomers could be successfully accounted for by using GIAO *ab initio* molecular orbital chemical shift calculations at the B3LYP/6-311G** level of theory on the B3LYP/6-31G* optimized geometries of a set of model compounds, **III'**, **IV'**, and **XV'**, which had H's as substituents on the cage carbons. However, neither similar calculations on the “carbons adjacent” carboranes nor comparisons with the spectra of carboranes having similar structures could successfully account for the ^{11}B NMR spectra of **XI**–**XIII**. It was speculated that the presence of two different substituents on the cage carbons of these compounds gives rise in solution to multiple isomers that would greatly complicate their NMR spectra.

Introduction

The syntheses of higher order borane and carborane cages are generally accomplished by atom insertion reactions or the fusion of smaller clusters.¹ Over 20 years ago, Grimes and co-workers reported the first metal-promoted oxidative face-to-face fusion reaction in the C₂B₄ carborane system.² In these reactions a transition metal sandwiched metallocarborane hydride of the type (R₂C₂B₄H₄)₂MH_x (M = Fe (*x* = 2), Co (*x* = 1); R = CH₃, C₂H₅, *n*-C₃H₇, CH₂C₆H₅) underwent mild air oxidation to produce 12-vertex tetracarborane clusters with the general formula, R₄C₄B₈H₈.^{3–6} The structures of the solid-state fusion products were found to be functions of the nature of R. When R = CH₃, the C₄B₈ cage had an distorted-icosahedral geometry in which all four carbon atoms were localized on the same side of the cluster face and linked to one another in a Z-shaped pattern (isomer GA),⁴ while when R = C₂H₅ the carbon face was more open such that the middle carbon–carbon bond was broken (isomer GB),⁵ when R = C₃H₇, mixtures of both GA and GB structures were found in the solid products.⁵ The solution NMR spectra of these compounds showed equilibrium mixtures of both GA and GB structures.⁵ Only when R = CH₂C₆H₅ was a stereochemically rigid structure of the type GB found in both the solid and solution phases.⁶ Because of the grouping of the carbon atoms on the same side of the cluster, these carboranes can be referred to as the “carbons adjacent” carborane isomers. We have recently reported the synthesis of several *closo*-carboranes of the form *closo*-1-(SiMe₃)-2-(R)-1,2-C₂B₄H₄ (R = SiMe₃, Me, H) by the oxidative cage closure of the respective dilithium complexed *nido*-carborane dianions [2-(SiMe₃)-3-(R)-2,3-C₂B₄H₄]²⁻ in the presence of NiCl₂⁷ and have explored their subsequent thermal rearrangements to the corresponding 1,6-isomers.⁸ These syntheses are of interest in that the *closo*-carboranes thus formed can be reductively opened to give dianionic *nido*-carborane isomers in which the cage carbons are separated by a boron atom, thereby furnishing new synthons for metallocarborane complexes in the 1,2,4-MC₂B₄ cage sys-

tem.⁹ During the reinvestigation of the oxidative cage closure reactions of the bis(trimethylsilyl)-substituted *nido*-2,3-C₂B₄-carboranes, we observed an accompanying oxidative cage fusion process that led to the formation of a novel tetracarborane isomer, 2,4,7,9-(SiMe₃)₄C₄B₈H₈, whose structure was based more on the cuboctahedron than on the icosahedron.¹⁰ This new geometry is of interest in that a cuboctahedral structure was proposed by Lipscomb for the key intermediate in the diamond–square–diamond (DSD) mechanism of the thermal conversion of *closo*-1,2-C₂B₁₀H₁₂ to *closo*-1,7-C₂B₁₀H₁₂.¹¹ 2,4,7,9-(SiMe₃)₄C₄B₈H₈ was found to be thermally unstable but did not isomerize to either of Grimes' isomers; moreover, the use of Grimes' method for the oxidative ligand fusion, involving the reaction of FeCl₂ with the monosodium salt of *nido*-2,3-(SiMe₃)₂-2,3-C₂B₄H₆, failed to produce the “carbons adjacent” analogues of (SiMe₃)₄C₄B₈H₈.¹⁰ This raises a fundamental question as to what factors are important in determining the structures of the oxidative fusion products of the C₂B₄ cages. The *nido*-carboranes used in our laboratories have trimethylsilyl groups on the cage carbons, while those of Grimes were alkyl-substituted compounds. Since the steric requirements of the cage carbon substituents have been shown to be important in the solution behavior of the C₄B₈ cages,⁶ an investigation of the steric effects of the cage-carbon substituents on the oxidative fusion reactions was undertaken. Specifically, it would be of interest to determine whether “carbons adjacent” C₄B₈ carboranes, similar to those described by Grimes, could be synthesized from the NiCl₂ reaction if one of the C-SiMe₃ moieties in the *nido*-2,3-(SiMe₃)₂-2,3-C₂B₄H₆ precursor was replaced by other groups of varying size, such as methyl, *n*-butyl, and *tert*-butyl moieties. Here we report the results of our extended investigation of the cage closure and cage fusion processes involving small-cage carborane ligands and nickel halides.

Experimental Section

Materials. 2,3-Bis(trimethylsilyl)-2,3-dicarba-*nido*-hexaborane(8) and 2-(trimethylsilyl)-3-methyl-2,3-dicarba-*nido*-hexaborane(8) were prepared by the methods of Hosmane et al.^{12,13} 1-(Trimethylsilyl)-1-hexyne (Me₃SiC≡C^{*n*}Bu) and 1-(trimethylsilyl)-3,3-dimethyl-1-butyne (Me₃SiC≡C^{*n*}Bu), purchased from Giese, Inc., were checked for purity before use by comparing their IR and boiling points with literature values. Mineral oil free NaH (Aldrich) and *tert*-butyllithium, *t*-BuLi (1.5 or 1.7 M solution in pentane obtained from Aldrich), were used as received. Prior to use, anhydrous NiCl₂ (Aldrich) was heated to 120 °C in vacuo to remove any trace quantity of moisture. Benzene, THF, and *n*-hexane were dried over

[†] Dedicated with all best wishes to Prof. Heinrich Nöth of Universität München on the occasion of his 70th birthday.

[‡] Present address: Department of Chemistry and Biochemistry, The Michael Faraday Laboratories, Northern Illinois University, DeKalb, IL 60115-2862. E-mail: nhosmane@niu.edu.

[§] Southern Methodist University.

^{||} Harvard University.

(1) For examples see: (a) Onak, T. In *Comprehensive Organometallic Chemistry II*; Abel, E. W., Stone, F. G. A., Wilkinson, G., Eds.; Elsevier: New York, 1995; Vol. 1, Chapter 6. (b) Wermer, J. R.; Shore, S. G. In *Advances in Boron and the Boranes*; Liebman, J. F., Greenberg, A., Williams, R. E., Eds.; VCH: New York, 1988; Chapter 2.

(2) (a) Maxwell, W. M.; Miller, V. R.; Grimes, R. N. *J. Am. Chem. Soc.* **1974**, *96*, 7116. (b) Maxwell, W. M.; Miller, V. R.; Grimes, R. N. *Inorg. Chem.* **1976**, *15*, 1343.

(3) (a) Maynard, R. B.; Grimes, R. N. *J. Am. Chem. Soc.* **1982**, *104*, 5983. (b) Grimes, R. N. *Adv. Inorg. Chem. Radiochem.* **1983**, *26*, 55.

(4) Freyberg, D. P.; Weiss, R.; Sinn, E.; Grimes, R. N. *Inorg. Chem.* **1977**, *16*, 1847.

(5) Venable, T. L.; Maynard, R. B.; Grimes, R. N. *J. Am. Chem. Soc.* **1984**, *106*, 6187.

(6) Spencer, J. T.; Pourian, M. R.; Butcher, R. J.; Sinn, E.; Grimes, R. N. *Organometallics* **1987**, *6*, 335.

(7) Hosmane, N. S.; Saxena, A. K.; Barreto, R. D.; Zhang, H.; Maguire, J. A.; Jia, L.; Wang, Y.; Oki, A. R.; Grover, K. V.; Whitten, S. J.; Dawson, K.; Tolle, M. A.; Siriwardane, U.; Demissie, T.; Fagner, J. S. *Organometallics* **1993**, *12*, 3001.

(8) Lu, K.-J.; Thomas, C. J.; Wang, Y.; Gray, T. G.; Maguire, J. A.; Hosmane, N. S.; Binder, H.; Wanitschek, M.; Borrmann, H.; Simon, H.; Oberhammer, H. *Chem. Eur. J.* **1997**, *3*, 1059.

(9) (a) Zhang, H.; Wang, Y.; Saxena, A. K.; Oki, A. R.; Maguire, J. A.; Hosmane, N. S. *Organometallics* **1993**, *12*, 3933. (b) Hosmane, N. S.; Jia, L.; Zhang, H.; Maguire, J. A. *Organometallics* **1994**, *13*, 1411. (c) Saxena, A. K.; Zhang, H.; Maguire, J. A.; Hosmane, N. S.; Cowley, A. H. *Angew. Chem., Int. Ed. Engl.* **1995**, *34*, 332. (d) Hosmane, N. S.; Saxena, A. K.; Lu, K.-J.; Maguire, J. A.; Zhang, H.; Wang, Y.; Thomas, C. J.; Zhu, D.; Grover, B. R.; Gray, T. G.; Eintracht, J. F. *Organometallics* **1995**, *14*, 5104.

(10) Hosmane, N. S.; Zhang, H.; Maguire, J. A.; Wang, Y.; Thomas, C. J.; Gray, T. G. *Angew. Chem., Int. Ed. Engl.* **1996**, *35*, 1000.

(11) (a) Lipscomb, W. N.; Britton, D. *J. Chem. Phys.* **1960**, *33*, 275. (b) Lipscomb, W. N. *Science* **1966**, *153*, 373.

(12) Hosmane, N. S.; Barreto, R. D. *Inorg. Synth.* **1992**, *29*, 89.

(13) (a) Hosmane, N. S.; Sirmokadam, N. N.; Mollenhauer, M. N. *J. Organomet. Chem.* **1985**, *279*, 359. (b) Hosmane, N. S.; Cowley, A. H.; Norman, N. C. *Organometallics* **1985**, *4*, 1194.

LiAlH₄ and doubly distilled before use. *N,N,N,N*-Tetramethylethylenediamine (TMEDA; Aldrich) was distilled in vacuo and stored over sodium metal.

Spectroscopic and Analytical Procedures. Proton, boron-11, and carbon-13 pulse Fourier transform NMR spectra at 200, 64.2, and 50.3 MHz, respectively, were recorded on an IBM-200 SY multinuclear NMR spectrometer. Infrared spectra were recorded on a Nicolet Magna-550 FT-IR spectrophotometer. Mass spectral determinations were performed at the Washington University Resource for Biomedical and Bioorganic Mass spectrometry, St. Louis, MO. Elemental analyses were obtained from E+R Microanalytical Laboratory, Inc., Corona, NY.

Synthetic Procedures. Except where otherwise indicated, all operations were conducted *in vacuo*. All room-temperature and sub-room-temperature experiments were carried out in Pyrex glass round-bottom flasks of 100–250 mL capacity, containing magnetic stirring bars and fitted with high-vacuum Teflon valves. All high-temperature experiments were carried out in Hoke stainless steel single-ended cylinders of 500 mL capacity (obtained from Tech Controls, Inc., Dallas, TX) fitted with forged body shutoff valves of 1/4 in. male npt and 1/4 in. Swagelok fittings (obtained from Texas Valve and Fitting Co., Dallas, TX). Nonvolatile substances were manipulated in either a drybox or evacuable glovebags under an atmosphere of dry nitrogen. All known compounds among the products were identified by comparing their infrared and/or NMR spectra with those of authentic samples.

Preparation of *nido*-2-(SiMe₃)-3-(R)-2,3-C₂B₄H₆ (R = *n*-Bu (I), *t*-Bu (II)). In a procedure identical with that reported by Hosmane *et al.*,^{12,13} pentaborane(9) (10.2 g, 162 mmol or 1.02 g, 16.2 mmol) and Me₃SiC≡C^{*n*}Bu (100 g, 648 mmol) or Me₃SiC≡C^{*t*}Bu (10.0 g, 64.9 mmol) were condensed at -196 °C into a 500 mL single-ended stainless steel reactor fitted with a high-vacuum Swagelok shutoff valve. The mixture was then warmed to room temperature and the lower half of the reactor maintained at a temperature of 140–150 °C by immersion in an oil bath for a period of approximately 3 days. After that time, the cylinder was reattached to the vacuum line through a 100 mL glass bulb and accumulated noncondensable gas (H₂) pumped out through a series of traps (two at 0 °C, one at -78 °C, and one at -196 °C) over a period of 10–12 h. Following the fractionation procedure described in the preparation of *nido*-2,3-(SiMe₃)₂-2,3-C₂B₄H₆,^{11,12} the cylinder was then slowly warmed to 140–150 °C using an oil bath and the volatile products fractionated through the trap system over a period of 3 days to afford pure *nido*-2-(SiMe₃)-3-(R)-2,3-C₂B₄H₆ (R = *n*-Bu (I), 11.0 g, 53.9 mmol; R = *t*-Bu (II), 1.5 g, 7.35 mmol), collected in the 0 °C traps. The yields, based on the pentaborane(9) consumed, were 33% and 45% for R = *n*-Bu and *t*-Bu, respectively. Unreacted Me₃SiC≡C-*n*-Bu (10 g) or Me₃SiC≡C-*t*-Bu (1.4 g) was collected in the -78 °C trap, while the -196 °C trap contained unreacted pentaborane(9) and Me₃SiH. Further fractionation of the contents of the -196 °C trap through -93 °C and -196 °C traps resulted in the recovery of the pentaborane(9) (2.49 g, 39.4 mmol or 0.18 g, 2.85 mmol) in the trap held at -93 °C, while the Me₃SiH (not measured) was in the -196 °C trap. The NMR and IR spectroscopic data for I and II are listed in Tables 1 and 2, respectively.

Syntheses of the (SiMe₃)₄C₄B₈H₈ "Carbons Apart" Tetracarbon Carborane Isomers III and IV. A 20 mL tetramethylethylenediamine (TMEDA) solution of *nido*-2,3-(SiMe₃)₂-2,3-C₂B₄H₆ (6 g, 27.3 mmol) was cooled to -78 °C, and *t*-BuLi (1.7 M in pentane, 54.6 mmol) was slowly added to this solution in vacuo, with constant stirring. When the addition was complete, the mixture was warmed slowly to room temperature and was held at that temperature for approximately 6 h to afford the solvated dilithiacarborane *closo*-*exo*-4,5-[(*u*-H)₂Li(TMEDA)]-1-Li(TMEDA)-2,3-(SiMe₃)₂-2,3-C₂B₄H₄, as described elsewhere.⁷ The solvent mixture was

removed in vacuo and the resulting dilithium compound (not measured) was redissolved in ~20 mL of benzene and then slowly added to anhydrous NiCl₂ (3.54 g; 27.3 mmol) at 0 °C. The resulting dark brown heterogeneous mixture was stirred for 12–15 h at room temperature and filtered in vacuo through a glass frit, and the residue was washed with warm benzene to collect a pale yellow filtrate. The volatile components of this filtrate were then fractionated over a period of 2¹/₂ days through a series of traps maintained at 0, -45, -78, and -196 °C, to afford the previously reported⁷ 1,2-bis(trimethylsilyl)-1,2-dicarba-*closo*-hexaborane(6), *closo*-1,2-(CSiMe₃)₂B₄H₄ (1.9 g, 8.7 mmol; 32% yield), in the U-trap held at -45 °C. The U-trap containing the *closo*-carborane was then removed and replaced by a clean U-trap and the pale brown residue remaining in the reaction flask was heated slowly to 110–120 °C, *in vacuo*, to collect a white crystalline solid of the fusion product (CSiMe₃)₄B₈H₈ (1.4 g; 25% yield) in the U-trap held at 0 °C. The solution NMR spectra of this solid material revealed it to be a 1:1 mixture of two isomers of (CSiMe₃)₄B₈H₈, III and IV (vide infra). Slow recrystallization from a 1:1 mixture of benzene and hexane gave colorless plates of *nido*-2,4,7,9-(SiMe₃)₄-2,4,7,9-C₄B₈H₈ (III; 0.65 g, 1.49 mmol; 11% yield; mp 95 °C). Anal. Found (calcd) for C₁₆H₄₄B₈Si₄(III): C, 44.19 (44.15); H, 10.33 (10.19); B, 19.96 (19.85). MS (*m/z* (%)): 435 (M⁺, 100), 73 (Me₃Si, 60). This isomer was found to be stable in air and soluble in both polar and nonpolar organic solvents. The solution remaining after the complete removal of III was concentrated to dryness to give a white residue, which was further purified by sublimation at 140–156 °C to afford colorless rectangular crystals of *nido*-2,4,6,12-(SiMe₃)₄-2,4,6,12-C₄B₈H₈ (IV; 0.72 g, 1.6 mmol; 12% yield; mp 68 °C). Anal. Found (calcd) for C₁₆H₄₄B₈Si₄(IV): C, 44.16 (44.15); H, 10.43 (10.19); B, 19.60 (19.85). MS (*m/z* (%)): 435 (M⁺, 100), 73 (Me₃Si, 58). Compound IV was found to be stable in air and soluble in both polar and nonpolar organic solvents. The NMR and IR spectroscopic data for III and IV are listed in Tables 1 and 2, respectively.

After the dark residue in the original reaction flask was heated to >165 °C, 0.41 g of a pale brown oil was obtained, which was partially characterized and found to be a physical mixture of *B*-Me- and/or *B*-*t*-Bu-substituted C₄B₈ carboranes. Attempts to separate this mixture were unsuccessful.

Thermal Rearrangement of III to IV. A 2.5 g (5.75 mmol) sample of III, dissolved in 2 mL of C₆D₆, was sealed in a Pyrex glass tube (8 mm diameter) in vacuo and then heated uniformly using an oil bath at 100 °C and monitored at regular intervals of time by NMR spectroscopy. The ¹¹B NMR spectrum of the solution indicated that complete conversion of III to IV took place after ca. 6 h of heating. When the conversion was complete, the tube was cut open and the solvent was removed under reduced pressure to obtain an off-white solid, which was purified by sublimation (25–70 °C at 10⁻⁵ mmHg) to obtain colorless rectangular crystals of IV (2.4 g, 5.5 mmol) in 96% yield.

Synthesis of *closo*-1-(SiMe₃)-2-(R)-1,2-C₂B₄H₄ (R = *n*-Bu (V), R = *t*-Bu (VI)) and 2,6-(R)₂-4,12-(SiMe₃)₂-2,4,6,12-C₄B₈H₈ (R = *n*-Bu (VII), *t*-Bu (VIII)). *nido*-2-(SiMe₃)-3-(R)-2,3-C₂B₄H₆ (R = *n*-Bu (I), 2.50 g, 12.3 mmol; R = *t*-Bu (II), 2.11 g, 10.4 mmol), dissolved in 10 mL of pentane, was poured, with stirring, into 14.5 mL (24.7 mmol) or 12 mL (20.4 mmol) of a solution of *t*-BuLi (1.7 M in pentane) in vacuo at -78 °C. The mixture was warmed to room temperature and stirred for 6–8 h to obtain a clear solution. This solution was then poured onto 1.6 g (12.3 mmol) or 1.4 g (10.8 mmol) of anhydrous NiCl₂ in vacuo at 0 °C, and the resulting heterogeneous mixture was stirred for an additional 24 h. Using the same procedures, temperatures, trap arrangements (0, -45, -78, and -196 °C), and times described above for the product separation in the syntheses of III and IV (vide supra), *closo*-1-(SiMe₃)-2-(R)-1,2-C₂B₄H₄ (R = *n*-Bu (V), 1.60 g, 7.9 mmol, 64% yield, bp 155–160 °C; R = *t*-Bu (VI), 1.45 g, 7.2 mmol, 69%, bp 150–155 °C)

Table 1. FT NMR Spectral Data^a

compd	δ , splitting, assign ^t ($^1J(^{11}\text{B}^1\text{H})$ or $^1J(^{13}\text{C}^1\text{H})$, Hz)	rel area
200.13 MHz ^1H NMR Data		
I	4.20–1.80, br, BH; 2.58, br, CH ₂ ; 1.73, br, CH ₂ ; 1.53, br, CH ₂ ; 1.03, s, CH ₃ ; 0.33, s, SiMe ₃ ; –2.01, br, BHB bridge	4:2:2:2:3:9:2
II	4.10–1.70, br, BH; 1.34, s, CMe ₃ ; 0.43, s, SiMe ₃ ; –1.90, br, BHB bridge	4:9:9:2
III	4.0–0.20, vvbr, BH; 0.17, s (br), SiMe ₃	1:4:5
IV	4.0–0.20, vvbr, BH; 0.16, s (br), SiMe ₃	1:4:5
V	2.29, br, BH; 1.66, br, CH ₂ ; 1.33, br, CH ₂ ; 1.14, br, CH ₂ ; 0.61, s, CH ₃ ; 0.42, s, SiMe ₃	4:2:2:2:3:9
VI	2.81, br q, BH; 1.37, s, CMe ₃ ; 0.44, s, SiMe ₃	4:9:9
VII	4.20, br, BH; 1.65, s, CH ₂ ; 1.20, s br, CH ₂ ; 0.84, s, CH ₃ ; 0.16, s, SiMe ₃	4:2:4:3:9
VIII	3.0–1.60, br, BH; 1.33, s, CMe ₃ ; 0.29, s, SiMe ₃	4:9:9
IX	2.40, br, BH; 2.10, br, CH ₂ ; 1.63, br, CH ₂ ; 1.19, br, CH ₂ ; 0.52, s, CH ₃ ; 0.37, SiMe ₃	4:2:2:2:3:9
X	2.78, q, BH; 1.31, s, CMe ₃ ; 0.36, s, SiMe ₃	4:9:9
XI	2.8–1.6, br, BH; 1.4, br s, CH ₂ ; 1.2, br s, CH ₂ ; 0.90, s, Me; 0.25, s, SiMe ₃ ; 0.20, s, SiMe ₃	4:2:4:3:4.5:4.5
XII	2.6–1.4, br, BH; 1.16, br s, CH ₂ ; 1.12, br s, CH ₂ ; 0.94, s, Me; 0.28, s, SiMe ₃ ; 0.21, s, SiMe ₃	4:2:4:3:4.5:4.5
XIII	3.33–1.3, vbr, BH; 1.36, br s, Me; 0.11, s, SiMe ₃	4:3:9
XIV	3.1–1.2, vbr, BH; 1.34, br s, Me; 0.09, s, SiMe ₃	4:3:9
XV	3.0–1.3, br, BH; 1.75, br, s, CH ₂ ; 1.06, br, m, CH ₂ ; 0.69, m, Me; 0.10, s, SiMe ₃	4:2:4:3:9
64.21 MHz ^{11}B NMR Data ^b		
I	1.10, br, basal B (unresolved); –2.89, d, basal B (109); –49.46, d, apical B (174)	1:2:1
II	–2.32, d, basal B (211); –49.62, d, apical B (125)	3:1
III	–30.18, d (162)	
IV	–5.57, d (147)	
V	7.08, d, equatorial B (160); –3.14, d, equatorial B (164); –12.02, d, axial B (180)	1:1:2
VI	8.21, d, equatorial B (160); –2.50, d, equatorial B (166); –11.99, d, axial B (180)	1:1:2
VII	–4.81, d (br) (unresolved)	
VIII	–5.33, d (br) (unresolved)	
IX	–14.60, d, equatorial B (184)	
X	–14.94, d, equatorial B (186)	
XI	10.42, d (br), (138); 3.67, d (113); 1.03, d (br), (unresolved); –7.49, d (br) (unresolved); –27.17, d (152); –30.49, d (147)	2:1:1:1:2:1
XII	14.28, d (br) (unresolved); 6.33, d (145); –0.23, d (127); –2.09, d (br), (unresolved); –21.89, d (150); –25.45, d (146)	1:2:2:1:1:1
XIII	7.93, d (br) (unresolved); 2.12, d (139); 4.79, d (br) (unresolved); –5.89, d (br) (unresolved); –22.46, d (155); –35.02, d (149)	1:1:2:2:1:1
XIV	–4.45, d (br), (148)	
XV	–7.76, vbr, ill-defined peak (unresolved)	
50.32 MHz ^{13}C NMR Data ^{a,c}		
I	149.06, s (br), cage carbons (CCSi); 133.90, s (br), cage carbons (CCB); 36.15, t, CH ₂ (123); 33.67, t, CH ₂ (125); 22.87, t, CH ₂ (120); 14.16, q, Me (125); 0.68, q, SiMe ₃ (120)	1:1:1:1:1:1:3
II	149.21, s (br), cage carbons (CCSi); 132.68, s, cage carbons (CCB); 30.2, q, C–Me ₃ (121); 28.1, s, C–Me ₃ ; 0.59, q, SiMe ₃ (119)	1:1:3:1:3
III	–1.1, q, SiMe ₃ (120); –33.32, s, cage carbons (CCSi)	3:1
IV	–1.4, q, SiMe ₃ (120); –11.41, s, cage carbons (CCSi)	3:1
V	74.70, s (br), cage carbons (CCSi); 66.58, s (br), cage carbons (CCB); 32.95, t, CH ₂ (128); 26.46, t, CH ₂ (127); 22.36, t, CH ₂ (120); 13.87, q, CH ₃ (119); –0.43, q, SiMe ₃ (118)	1:1:1:1:1:1:3
VI	87.1, s, cage carbons (CCSi); 70.8, s, cage carbons (CCB); 29.9, q, C–Me ₃ (121); 26.1, s, C–Me ₃ ; 0.59, q, SiMe ₃ (120)	1:1:3:1:3
VII	38.11, t, CH ₂ (125); 32.82, t, CH ₂ (125); 22.74, t, CH ₂ (129); 17.11, s, cage carbons (CCSi); 13.82, q, Me (125); –0.95, q, SiMe ₃ (120); –6.97, s, cage carbons (CCB)	1:1:1:1:1:3:1
VIII	29.1, q, C–Me ₃ (123); 26.9, s, C–Me ₃ ; 18.03, s, cage carbons (CCSi); 0.76, q, SiMe ₃ (119); –6.11, s, cage carbons (CCB)	3:1:1:3:1
IX	110.04, s, cage-C–SiMe ₃ ; 81.29, s, cage-C–Bu; 32.86, t, CH ₂ , $^1J(\text{CH}) = 134.28$ Hz; 27.48, t, CH ₂ , $^1J(\text{CH}) = 126.75$ Hz; 22.45, t, CH ₂ , $^1J(\text{CH}) = 126.76$ Hz; 13.91, q, Me, $^1J(\text{CH}) = 124.6$ Hz; –0.52, q, SiMe ₃ , $^1J(\text{CH}) = 118.16$ Hz	1:1:1:1:1:1:3
X	121.8, s, cage-C–SiMe ₃ ; 79.5, s, cage-C–CMe ₃ ; 31.62, q, C–Me ₃ , $^1J(\text{CH}) = 120.3$ Hz; 25.73, s, C–Me ₃ ; –0.52, q, Si–Me ₃ , $^1J(\text{CH}) = 118.2$ Hz	1:1:3:1:3
XI	39.75, t, CH ₂ (131); 33.95, t, CH ₂ (121); 23.22, t, CH ₂ (121); 22.91, s, cage carbons (CCSi); 13.85, q, Me (131); 3.03, s, cage carbons (CCB); 0.44, q, SiMe ₃ (119)	1:1:1:1:1:1:3
XII	39.50, t, CH ₂ (126); 31.69, t, CH ₂ (125); 22.76, t, CH ₂ (126); 17.02, s, cage carbons (CCSi); 14.02, q, Me (125); –0.72, q, SiMe ₃ (120); –7.19, s, cage carbons (CCB)	1:1:1:1:1:3:1
XIII	29.08, s, cage carbons (CCSi); 23.92, q (br), Me (131); 16.31, s, cage carbons (CCB); 0.33, q (br), SiMe ₃ (119)	1:1:1:3
XIV	35.21, q (br), Me (129); 9.17, s, cage carbons (CCSi); 1.57, q (br), SiMe ₃ (119); –2.39, s, cage carbons (CCB)	1:1:3:1
XV	33.81, t, CH ₂ (125); 30.92, t, CH ₂ (124); 22.97, t, CH ₂ (129); 14.2, s, cage carbons (CCSi); 13.76, q, Me (126); –0.20, q, SiMe ₃ (119); –0.52, q, SiMe ₃ (120); –5.89, s, cage carbons (CCB)	1:1:1:1:1:1.5:1:5:1

^a C₆D₆ was used as solvent and as an internal standard of δ 7.15 ppm (in the ^1H NMR spectra) and δ 128.0 ppm (in the ^{13}C NMR spectra) for compounds, with a positive sign indicating a downfield shift. Legend: s = singlet, d = doublet, t = triplet, q = quartet, v = very, br = broad. ^b Shifts relative to external BF₃·OEt₂. ^c Since relaxations of the quaternary and the cage carbons are slower than that of a protonated C, the relative areas of these carbons could not be measured accurately.

was obtained in reasonably high purities in the –45 °C trap. After removal of the *closo*-carboranes, the dark residue

remaining in the flask was heated to 140 °C in vacuo to collect, in the 0 °C trap, the “carbons apart” carboranes *nido*-2,6-(R)₂-

Table 2. Infrared Absorptions (cm⁻¹)^a

I	2958 (vs, $\nu(\text{CH})$), 2930 (vs, $\nu(\text{CH})$), 2903 (s, $\nu(\text{CH})$), 2882 (s), 2868 (s), 2602 (vs, $\nu(\text{BH})$), 1945 (w, $\nu(\text{BH}_{\text{bridge}})$), 1875 (vw, sh), 1478 (s, sh), 1470 (s), 1414 (w), 1386 (w), 1344 (w), 1270 (vs), 1176 (w), 1106 (m), 1022 (w), 987 (w), 952 (m), 924 (m), 847 (vs), 757 (s), 750 (s), 694 (m), 666 (m), 638 (m), 526 (vw)
II	2966 (vs, $\nu(\text{CH})$), 2908 (m), 2875 (m), 2605 (vs, $\nu(\text{BH})$), 1960 (vw, $\nu(\text{BH}_{\text{bridge}})$), 1486 (m), 1473 (m), 1394 (w), 1374 (s), 1262 (vs), 1210 (m), 1175 (s), 1085 (m), 1019 (m), 979 (w), 900 (m), 845 (vs), 762 (s), 703 (m), 643 (m), 624 (m)
III	2280 (vs, $\nu(\text{BH})$), 2269 (s, $\nu(\text{BH})$), 2253 (s, $\nu(\text{BH})$), 1358 (w), 1385 (vw), 1330 (s), 1166 (vw), 1095 (vw), 910 (vs, vbr), 814 (vs), 733 (vs, vbr), 651 (vs), 507 (vs), 496 (vs), 427 (s)
IV	2963 (s, $\nu(\text{CH})$), 2901 (w, $\nu(\text{CH})$), 2580 (s, $\nu(\text{BH})$), 2539 (m, $\nu(\text{BH})$), 1409 (vw), 1249 (s), 1207 (w), 1135 (m), 1099 (w), 1023 (w), 989 (w), 975 (w), 961 (w), 938 (w), 893 (s), 881 (m), 845 (vs), 781 (m), 752 (m), 689 (m), 641 (w), 632 (w), 591 (w), 481 (w)
V	2960 (vs, $\nu(\text{CH})$), 2881 (s), 2631 (s, $\nu(\text{BH})$), 1473 (w), 1368 (w), 1256 (m), 1117 (w), 927 (vw), 848 (vs), 775 (vw), 644 (vw)
VI	2964 (vs, $\nu(\text{CH})$), 2902 (w), 2868 (w), 2635 (vs, $\nu(\text{BH})$), 1479 (w), 1464 (w), 1409 (vw), 1398 (vw), 1371 (m), 1254 (vs), 1203 (s), 1073 (w), 1026 (vw), 890 (m), 855 (vs), 843 (vs), 796 (w), 758 (m), 739 (vw), 701 (w), 634 (m), 417 (w)
VII	2958 (vs, $\nu(\text{CH})$), 2930 (s), 2901 (w), 2874 (w), 2860 (m), 2585 (s, $\nu(\text{BH})$), 2526 (s, $\nu(\text{BH})$), 1467 (w), 1458 (w), 1406 (vw), 1381 (vw), 1364 (vw), 1303 (w), 1254 (vs), 1219 (w), 1161 (m), 1139 (m), 1099 (s), 1026 (vw), 980 (w), 963 (m), 935 (w), 891 (s), 848 (vs), 807 (m), 777 (m), 753 (m), 730 (w), 692 (m), 662 (w), 627 (m)
VIII	2969 (vs, $\nu(\text{CH})$), 2910 (m), 2873 (m), 2610 (vs, $\nu(\text{BH})$), 1486 (m), 1475 (sh), 1380 (w), 1372 (s), 1260 (vs), 1210 (sh), 1177 (s), 1085 (m), 1019 (m), 976 (w), 910 (m), 845 (vs), 762 (s), 709 (m), 643 (m), 621 (m)
IX	2962 (vs, $\nu(\text{CH})$), 2934 (vs), 2875 (vs), 2861 (vs), 2797 (w), 2735 (vw), 2638 (vs, $\nu(\text{BH})$), 1466 (vs), 1442 (s), 1407 (s), 1381 (s), 1328 (m), 1311 (m), 1293 (s), 1253 (vs), 1196 (vs), 1118 (s), 1052 (vs), 987 (w), 972 (w), 938 (m), 894 (vs), 845 (vs), 755 (vs), 701 (s), 659 (w), 632 (vs), 530 (vw), 504 (vw), 435 (w), 413 (s)
X	2987 (vs, $\nu(\text{CH})$), 2907 (s), 2875 (s), 2637 (vs, $\nu(\text{BH})$), 1486 (m), 1479 (s), 1407 (w), 1413 (w), 1374 (vs), 1268 (vs), 1209 (vs), 1077 (s), 1031 (m), 893 (s), 860 (vs), 847 (vs), 801 (m), 764 (s), 742 (w), 702 (s), 636 (s), 432 (s)
XI	2966 (s, s), 2875 (w, s) ($\nu(\text{CH})$), 2578 (s, s) ($\nu(\text{BH})$), 2394 (w, s), 2282 (s, s), 2229 (w, sh), 1624 (m, s), 1466 (m, s), 1341 (s, s), 1262 (vs, s), 1137 (m, s), 1097 (m, s), 854 (vs, s), 808 (s, s), 762 (m, s), 689 (w, s), 623 (w, s), 512 (s), 485 (m, s)
XII	2978 (vs), 2944 (s, sh), 2908 (sh), 2872 (vs, br) ($\nu(\text{CH})$), 2614 (vs), 2508 (sh) ($\nu(\text{BH})$), 2105 (w), 1940 (w, br), 1623 (m, s), 1469 (m, s), 1338 (s), 1257 (vs, s), 1075 (s), 1015 (m), 965 (w), 918 (s), 846 (vvs), 810 (m), 757 (m, s), 695 (m, s), 641 (w, s)
XIII	2957 (vs), 2905 (s, sh), 2869 (m, sh) ($\nu(\text{CH})$), 2587 (s), 2530 (sh) ($\nu(\text{BH})$), 1462 (w), 1416 (m), 1370 (m, s), 1344 (m, br), 1252 (vs, s), 1103 (w, sh), 1082 (w, br), 903 (sh), 846 (vvs), 807 (m), 764 (w, s), 697 (w, s), 636 (vw, s)
XIV	2967 (s), 2934 (s, sh), 2907 (w, sh), 2875 (w, sh) ($\nu(\text{CH})$), 2591 (vs), 2526 (s, s) ($\nu(\text{BH})$), 1459 (m, s), 1407 (m, s), 1367 (w), 1255 (vs, s), 1170 (m, s), 1104 (m, s), 1077 (m, s), 1012 (m), 965 (w), 840 (vvs), 807 (sh), 696 (m, s), 631 (w, s)

^a C₆D₆ was used as solvent and reference standard. Legend: v = very, s = strong or sharp, m = medium, w = weak, sh = shoulder, br = broad.

4,12-(SiMe₃)₂-2,4,6,12-C₄B₈H₈ (R = *n*-Bu (**VII**), 0.35 g, 0.87 mmol, 14% yield; R = *t*-Bu (**VIII**), 0.28 g, 0.69 mmol, 13% yield). Compound **VII** was a colorless crystalline solid (mp 75–76 °C), while **VIII** was a highly viscous off-white oil (bp 183–185 °C). Anal. Found (calcd) for C₉H₂₂B₄Si (**V**): C, 53.93 (53.62); H, 11.31 (10.99); B, 21.68 (21.45). Found (calcd) for C₉H₂₂B₄Si (**VI**): C, 53.81 (53.62); H, 11.22 (10.99); B, 21.39 (21.45). Found (calcd) for C₁₈H₄₄B₈Si₂ (**VII**): C, 53.72 (53.62); H, 11.03 (10.99); B, 21.78 (21.45). MS for **VII** (*m/z*): 403 (M⁺, 23%), 188 (M⁺ – Me, 100%). Anal. Found (calcd) for C₁₈H₄₄B₈Si₂ (**VIII**): C, 53.68 (53.62); H, 11.06 (10.99); B, 21.38 (21.45). MS for **VIII** (*m/z*): 403 (M⁺, 24%), 188 (M⁺ – Me, 100%), 73 (Me₃Si, 71%). The NMR and IR spectroscopic data for **V–VIII** are listed in Tables 1 and 2, respectively.

Thermal Rearrangement of *closo*-1-(SiMe₃)₂-2-(R)-1,2-C₂B₄H₄ to *closo*-1-(SiMe₃)₆-(R)-1,6-C₂B₄H₄ (R = *n*-Bu (IX**), *t*-Bu (**X**)).** A neat sample of the *closo*-carborane *closo*-1-(SiMe₃)₂-2-(R)-1,2-C₂B₄H₄ (R = *n*-Bu (**V**), 2.5 g, 12.4 mmol; R = *t*-Bu (**VI**), 2.5 g, 12.4 mmol) was sealed in vacuo in a Pyrex glass tube (8 mm diameter) and heated slowly in a furnace for varying lengths of time. The reaction was followed by monitoring changes in the ¹¹B NMR spectrum of the sample. The time–temperature studies showed that the optimum conditions for the complete conversion of the 1,2-carborane to its 1,6-isomer was 4–5 h at a temperature range of 250–255 °C. After the determined period of time, the reaction was quenched by cooling to –196 °C. The reaction tube was then quickly transferred to a glovebag filled with dry nitrogen and cut open, and the contents were emptied into a flask (15 mL capacity) fitted with a Teflon stopcock; the flask was attached to a vacuum line and fractionated through a series of traps held at 0, –45, –78, and –196 °C. The fraction collected in the –45 °C trap was identified as *closo*-1-(SiMe₃)₆-(R)-1,6-C₂B₄H₄ (R = *n*-Bu (**IX**), 1.90 g, 9.4 mmol, 76% yield; R = *t*-Bu (**X**), 1.8 g, 8.9 mmol, 72% yield). The contents of the 0 °C trap were found to be mixtures of several products, including small amounts of the 1,2- and 1,6-isomers that did not pass through the trap. After removal of all volatiles a small quantity of an intractable, brown amorphous solid that remained in the flask

could not be further characterized and was therefore discarded. Anal. Found (calcd) for C₉H₂₂B₄Si (**IX**): C, 53.80 (53.62); H, 10.95 (10.99); B, 21.28 (21.45). Found (calcd) for C₉H₂₂B₄Si (**X**): C, 53.79 (53.62); H, 11.17 (10.99); B, 21.83 (21.45). MS for **IX**: 202 (M⁺, 5%), 187 (M – Me, 100%). MS for **X**: 202 (M⁺, 4%), 187 (M – Me, 100%). The NMR and IR spectral data for **IX** and **X** are listed in Tables 1 and 2, respectively.

Synthesis of the “Carbons Apart” *nido*-2,4,6,12-(SiMe₃)₄-2,4,6,12-C₄B₈H₈ (IV**) from Full-Sandwich Chromacarboranes.** The chromium(III) sandwich complex {Li(THF)₄}⁺-{1,1'-*commo*-Cr[2,3-(SiMe₃)₂-2,3-C₂B₄H₄]₂}⁻ was prepared by the room-temperature reaction of a THF solution of the Na⁺/Li⁺ complexed [2,3-(SiMe₃)₂-2,3-C₂B₄H₄]²⁻ dianion (14.5 mmol) with a benzene solution of anhydrous CrCl₃ (7.27 mmol), following the literature procedure.¹⁴ Instead of isolating and recrystallizing the intermediate chromacarborane, the THF/benzene solvent was removed from the reaction mixture to collect a dark reddish brown solid that was treated with a solvent mixture (1:1) of THF and hexane, and the entire contents of the flask were poured directly onto anhydrous PbCl₂ (7.27 mmol) at room temperature in vacuo. The resulting dark red heterogeneous mixture was stirred at room temperature for 3–4 days. The solvent was then removed in vacuo to give a dark red residue, which was slowly heated to 140–160 °C; the contents slowly sublimed at that temperature through traps held at 15 and 0 °C. The previously reported Cr(IV) sandwich complex, 1,1'-*commo*-Cr[2,3-(SiMe₃)₂-2,3-C₂B₄H₄]₂ (1.14 g, 4.68 mmol, 64% yield) was collected in the 15 °C trap,¹⁴ while the “carbons apart” tetracarbon carborane *nido*-2,4,6,12-(SiMe₃)₄-2,4,6,12-C₄B₈H₈ (**IV**; 0.94 g; 2.16 mmol, 30% yield) was collected in the 0 °C trap.

Synthesis of the “Carbons Adjacent” *nido*-1,4-(SiMe₃)₂-2,3-(*n*-Bu)₂-1,2,3,4-C₄B₈H₈ (XI**).** An *n*-hexane solution (15–20 mL) of *nido*-2-(SiMe₃)₃-3-(*n*-Bu)-C₂B₄H₄ (**I**; 6.06 g, 29.8 mmol) was slowly added to 19.9 mL of a pentane solution of *t*-BuLi

(14) Oki, A. R.; Zhang, H.; Maguire, J. A.; Hosmane, N. S.; Ro, H.; Hatfield, W. E.; Moscherosch, M.; Kaim, W. *Organometallics* **1992**, *11*, 4202.

(1.5 M, 29.8 mmol) in vacuo at $-78\text{ }^{\circ}\text{C}$, and the resulting mixture was slowly warmed to room temperature with constant stirring over a period of 4 h; this resulted in the formation of a solution of the corresponding monolithium compound of the $[nido-2-(\text{SiMe}_3)_3-3-(n\text{-Bu})\text{-C}_2\text{B}_4\text{H}_5]^-$ anion. The solution was then slowly poured onto anhydrous NiCl_2 (3.9 g, 30.0 mmol) that was suspended in 5 mL of *n*-hexane in vacuo at $0\text{ }^{\circ}\text{C}$. The resulting brown heterogeneous mixture was stirred for 24 h at room temperature. The solvent was then removed from the mixture at $-45\text{ }^{\circ}\text{C}$ in vacuo, leaving in the flask a dark brown residue that was subsequently heated slowly to $115\text{--}120\text{ }^{\circ}\text{C}$ in vacuo, during which time a large amount of liquid was collected in a U-trap held at $0\text{ }^{\circ}\text{C}$; the contents of this U-trap were later analyzed and found to be a mixture of **VII** and **I** (see below). After complete removal of all the volatile products, the U-trap at $0\text{ }^{\circ}\text{C}$ was replaced and the dark residue in the flask was heated further to $140\text{ }^{\circ}\text{C}$ in vacuo to collect a colorless crystalline solid, identified as the "carbons adjacent" *nido*-1,4-(SiMe_3)₂-2,3-(*n*-Bu)₂-1,2,3,4- $\text{C}_4\text{B}_8\text{H}_8$ (**XI**; 2.2 g, 5.45 mmol, 37% yield, mp $55\text{--}56\text{ }^{\circ}\text{C}$), as a sublimable product on the inside wall of the U-trap at $0\text{ }^{\circ}\text{C}$. Compound **XI** is stable in air and is soluble in both polar and nonpolar organic solvents. Anal. Found (calcd) for $\text{C}_{18}\text{H}_{44}\text{B}_8\text{Si}_2$ (**XI**): C, 53.87 (53.62); H, 11.08 (10.99). The NMR and IR spectroscopic data for **XI** are listed in Tables 1 and 2, respectively.

The liquid that was collected in the original U-trap was warmed to room temperature and fractionated through a series of U-traps held at 0 , -45 , and $-196\text{ }^{\circ}\text{C}$, respectively, *in vacuo*. This second fractionation resulted in the isolation of a colorless liquid, in the trap held at $-45\text{ }^{\circ}\text{C}$, which was identified as *nido*-2-(SiMe_3)₃-3-(*n*-Bu)-2,3- $\text{C}_2\text{B}_4\text{H}_6$ (2.3 g, 11.3 mmol). A viscous liquid, collected in the $0\text{ }^{\circ}\text{C}$ trap, was slowly crystallized on standing over a period of 7–8 days to give the "carbons apart" *nido*-2,7-(SiMe_3)₂-4,9-(*n*-Bu)₂-2,4,7,9- $\text{C}_4\text{B}_8\text{H}_8$ (**VII**; 1.1 g, 2.73 mmol, 18%).

Synthesis of the "Carbons Adjacent" *nido*-2,8-(SiMe_3)₂-3,9-(*n*-Bu)₂-2,3,8,9- $\text{C}_4\text{B}_8\text{H}_8$ (XII**).** During the resublimation of **VII** in one of the syntheses, involving the reaction of 34.9 mmol of **I**, a dark red viscous liquid was obtained along with solid **VII** in the U-trap held at $0\text{ }^{\circ}\text{C}$. After removal of **VII**, the liquid was allowed to stand in a vacuum flask in a cool place over a period of 7 days, during which time a slow crystallization of the liquid took place. After additional standing over a 3–4 week period, 0.29 g (0.71 mmol, 4% yield) of a crystalline solid, identified as a new isomeric form of the "carbons adjacent" tetracarborane *nido*-2,8-(SiMe_3)₂-3,9-(*n*-Bu)₂-2,3,8,9- $\text{C}_4\text{B}_8\text{H}_8$ (**XII**; mp $60\text{--}62\text{ }^{\circ}\text{C}$; stable in air; soluble in both polar and nonpolar organic solvents) was obtained. Anal. Found (calcd) for $\text{C}_{18}\text{H}_{44}\text{B}_8\text{Si}_2$ (**XII**): C, 53.67 (53.62); H, 11.03 (10.99). The NMR and IR spectroscopic data for **XII** are listed in Tables 1 and 2, respectively.

One-Pot Synthesis of the "Carbons Adjacent" *nido*-(SiMe_3)₂(Me)₂- $\text{C}_4\text{B}_8\text{H}_8$ (XIII**) and the "Carbons Apart" *nido*-2,6-(Me)₂-4,12-(SiMe_3)₂-2,4,6,12- $\text{C}_4\text{B}_8\text{H}_8$ (**XIV**).** In a procedure identical with that employed above for **VII** and **VIII**, 30.95 mmol (5.0 g) of *nido*-2-(SiMe_3)₃-3-(Me)-2,3- $\text{C}_2\text{B}_4\text{H}_6$, dissolved in hexane, was reacted with 62.19 mmol of *t*-BuLi (36.58 mL of 1.7 M in pentane) at $0\text{--}25\text{ }^{\circ}\text{C}$ for 4 h, to produce the unsolvated dilithiacarborane *closo-exo*-4,5-[(*u*-H)₂Li]-1-Li-2-(SiMe_3)₃-3-(Me)-2,3- $\text{C}_2\text{B}_4\text{H}_4$.⁷ Without isolation, the solution of this dilithiacarborane was slowly added in vacuo to a suspension of anhydrous NiCl_2 (3.94 g, 30.40 mmol) in hexane at room temperature and the resulting mixture was stirred constantly for 24 h. With the identical workup procedures employed for **VII** and **VIII**, 2.67 g (16.69 mmol, 54% yield) of *closo*-1-(SiMe_3)₂-2-(Me)-1,2- $\text{C}_2\text{B}_4\text{H}_4$ was collected in a U-trap maintained at $-45\text{ }^{\circ}\text{C}$. In the $0\text{ }^{\circ}\text{C}$ trap, a thick colorless viscous liquid was collected that was identified by exact mass measurement as (Me)₂(SiMe_3)₂- $\text{C}_4\text{B}_8\text{H}_8$ (1.84 g, 5.73 mmol, 37% yield) ($^{12}\text{C}_{12}\text{-}^1\text{H}_{34}\text{B}_8\text{Si}_2$ (M), found (calcd) m/z 322.2943 (322.2949); $^{12}\text{C}_{12}\text{-}$

$^1\text{H}_{34}\text{B}_8\text{Si}_2$ (M^+), found (calcd) m/z 321.2979 (321.2956)). Since the ^{11}B NMR spectra indicated the presence of more than one isomer of the tetracarborane, the liquid in the $0\text{ }^{\circ}\text{C}$ trap was further fractionated in vacuo slowly over a period of 7–8 days by warming the trap containing the liquid to room temperature and then allowing any volatiles to pass through a series of traps held at 0 , -78 , and $-196\text{ }^{\circ}\text{C}$. Although the complete separation was not possible, the trap at $0\text{ }^{\circ}\text{C}$ collected a small amount (0.59 g, 1.84 mmol) of a C_4B_8 isomer, identified by its ^1H and ^{11}B NMR spectra as the new "carbons adjacent" carborane (SiMe_3)₂(Me)₂- $\text{C}_4\text{B}_8\text{H}_8$ (**XIII**) in 12% yield. Anal. Found (calcd) for $\text{C}_{12}\text{H}_{34}\text{B}_8\text{Si}_2$ (**XIII**): C, 44.87 (44.89); H, 10.88 (10.67). The residue remaining after 8 days of fractionating at room temperature was then heated to $160\text{ }^{\circ}\text{C}$ for 24 h, which produced the "carbons apart" *nido*-2,6-(Me)₂-4,12-(SiMe_3)₂-2,4,6,12- $\text{C}_4\text{B}_8\text{H}_8$ (**XIV**; 1.22 g, 3.8 mmol), as characterized by a single broad doublet in its proton-coupled ^{11}B NMR spectrum (see Table 1). Anal. Found (calcd) for $\text{C}_{12}\text{H}_{34}\text{B}_8\text{Si}_2$ (**XIV**): C, 45.03 (44.89); H, 10.78 (10.67). Isomers **XIII** and **XIV** are soluble in polar and nonpolar organic solvents; their NMR and IR spectroscopic data are listed in Tables 1 and 2, respectively.

Synthesis of "Carbons Apart" *nido*-1-Br-2,6-(*n*-Bu)₂-4,12-(SiMe_3)₂-2,4,6,12- $\text{C}_4\text{B}_8\text{H}_8$ (XV**).** A 6.2 mmol (1.0 g) sample of Br_2 was dissolved in 30 mL of *n*-hexane, and the resulting reddish brown solution was slowly added in vacuo to 50 mL of an *n*-hexane solution of *nido*-2,6-(*n*-Bu)₂-4,12-(SiMe_3)₂-2,4,6,12- $\text{C}_4\text{B}_8\text{H}_8$ (**VII**; 1.21 g, 3.0 mmol) at liquid-nitrogen temperature. The resulting solution was slowly warmed to $0\text{ }^{\circ}\text{C}$ with constant stirring and was stirred further at this temperature overnight; during this time the solution became colorless. The solvent was then removed in vacuo, and the resulting off-white residue was heated to $180\text{ }^{\circ}\text{C}$ in vacuo to collect a colorless oil in a detachable U-trap held at $0\text{ }^{\circ}\text{C}$. After this U-trap was left in a cool place over a period of 7–8 days, the oily liquid was completely converted to a colorless crystalline solid, identified as the mono-B-brominated "carbons apart" tetracarborane *nido*-1-Br-2,6-(*n*-Bu)₂-4,12-(SiMe_3)₂-2,4,6,12- $\text{C}_4\text{B}_8\text{H}_8$ (**XV**; 0.67 g, 1.39 mmol, 46% yield; mp $75\text{--}76\text{ }^{\circ}\text{C}$). This compound was later recrystallized from its hexane solution for X-ray analysis. Anal. Found (calcd) for $\text{C}_{18}\text{H}_{43}\text{B}_8\text{BrSi}_2$ (**XV**): C, 48.52 (48.03); H, 9.35 (9.60). Compound **XV** is soluble in both polar and nonpolar organic solvents. The NMR and IR spectroscopic data for **XV** are listed in Tables 1 and 2, respectively.

A dark residue that remained in the original flask after distillation/sublimation was not very soluble in either polar or nonpolar solvents; the NMR spectra of its solution showed several unidentifiable peaks, indicating that some of the original compound may have undergone further bromination of the cage and/or fragmentation during the bromination reaction. Since this residue could not be further characterized or separated, it was discarded.

X-ray Analyses of **III, **IV**, **XI**, **XII**, and **XV**.** Colorless crystals of **III**, **IV**, **XI**, and **XII** were grown by vacuum sublimation onto glass surfaces in 8 mm tubes, while suitable crystals of **XV** were grown slowly from its *n*-hexane solution. The crystals were all coated with mineral oil in the drybox and mounted on a Siemens R3m/V diffractometer. Final unit cell parameters, given in Table 3, were obtained by least-squares fits of 24 accurately centered reflections, and the intensity data were collected at $220\text{--}230\text{ K}$ in the ranges $3.5 \leq 2\theta \leq 44.0^\circ$, $3.0 \leq 2\theta \leq 35.0^\circ$, $3.0 \leq 2\theta \leq 44.0^\circ$, $3.0 \leq 2\theta \leq 44.0^\circ$, and $7.0 \leq 2\theta \leq 45.0^\circ$ for **III**, **IV**, **XI**, **XII**, and **XV**, respectively. Three standard reflections that were periodically monitored during the data collection showed no significant change in intensity; the data were corrected for Lorentz and polarization effects. The structures were solved by direct or heavy-atom methods using the SHELXTL-Plus package of programs.¹⁵ Full-matrix least-squares refinements were performed, and all non-H atoms were refined anisotropically. The scattering factors, with anomalous dispersion corrections for

Table 3. Crystallographic Data^a for **III**, **IV**, **XI**, **XII**, and **XV**

	III	IV	XI	XII	XV
formula	C ₁₆ H ₄₄ B ₈ Si ₄	C ₁₆ H ₄₄ B ₈ Si ₄	C ₁₈ H ₄₄ B ₈ Si ₂	C ₁₈ H ₄₄ B ₈ Si ₂	C ₁₈ H ₄₃ B ₈ BrSi ₂
fw	435.4	435.4	403.2	403.2	482.1
space group	P2 ₁ /c	P1	P2 ₁ /m	Pbca	P2 ₁ /m
a, Å	9.628(2)	19.345(5)	8.385(10)	16.465(2)	9.8390(10)
b, Å	7.333(2)	19.577(4)	14.213(2)	17.225(2)	13.9250(10)
c, Å	19.924(5)	24.439(5)	11.422(2)	18.898(2)	10.7090(10)
α, deg		79.04(2)			
β, deg	93.46(2)	80.29(2)	103.150(10)		108.190(10)
γ, deg		89.63(2)			
V, Å ³	1404.0(6)	8953(4)	1325.5(3)	5359.7(11)	1394.1(2)
Z	2	12	2	8	2
D _{calcd} , g cm ⁻³	1.030	0.969	1.010	0.999	1.148
abs coeff, mm ⁻¹	0.214	0.202	0.137	0.135	1.565
crystal dmns, mm	0.30 × 0.35 × 0.10	0.20 × 0.25 × 0.10	0.20 × 0.30 × 0.10	0.40 × 0.30 × 0.05	0.40 × 0.35 × 0.20
scan type	ω	ω	2θ-θ	2θ-θ	ω
2θ range, deg	3.5–44.0	3.0–35.0	3.0–44.0	3.0–44.0	7.0–45
T, K	230	230	220	228	228
decay, %	0	0	0	0	0
no. of data collected	1841	11871	1832	3275	1910
no. of obsd rflns, F > 6.0σ(F)	1431	9455 ^d	1331	1554	1401
no. of parameters refined	216	1397	172	253	149
GOF	1.12	1.05	1.45	1.85	1.20
Δρ _{max,min} , e Å ⁻³	0.21, -0.13	1.4, -0.30	0.18, -0.41	0.26, -0.34	0.36, -0.26
R ^b	0.029	0.097	0.049	0.065	0.032
R _w ^c	0.040	0.238 ^e	0.065	0.090	0.048

^a Graphite-monochromatized Mo Kα radiation, λ = 0.710 73 Å. ^b R = Σ||F_o - |F_c||/Σ|F_o|; R_w = [Σw(F_o - F_c)²/Σw(F_o)²]^{1/2}. ^c w = 1/[σ²(F_o) + 0.001F_o²]. ^d Observed reflections F > 0.0σ(F). ^e w = 1/[σ²(F_o)² + (0.1431ρ)² + 30.74ρ], ρ = [(F_o)² + 2(F_c)²]/3.

heavy atoms, were taken from ref 16. Methyl and methylene H atoms in all structures were calculated using a riding model. Cage H atoms were located in difference Fourier maps, and except for **III**, they were not refined. Statistically, **XI** possesses a mirror plane passing through atoms C(1), C(4), B(7), B(9), Si(1), Si(2), C(22), and C(24). Atoms C(2) and C(3), along with their respective mirror images, are disordered; C(11) and C(11') are also disordered with an occupancy of 50% for each site. The final cycles of refinements of **III**, **XI**, **XII**, and **XV** converged at R = 0.029, 0.049, 0.065, and 0.032, R_w = 0.040, 0.065, 0.090, and 0.048, and GOF = 1.12, 1.45, 1.85, and 1.20, respectively. Selected bond distances and bond angles are listed in Table 4. Problems were encountered in the refinement of **IV**; despite repeated recrystallizations and sample preparation, the values of R in the final refinements of this compound were significantly higher than the others (R = 0.097 and R_w = 0.238; see Table 3). The analyses showed there to be six crystallographically independent molecules in the unit cell of **IV**. Repeated syntheses and recrystallizations by us and other groups, as well as studies at 163 K, gave essentially the same results.¹⁷ Because of the uncertainty in the structure, the bond distances and angles of **IV** are not included in Table 4 but can be found in the Supporting Material.

Calculations

Approximate density functional theory (DFT) ab initio molecular orbital calculations at several different levels of theory were carried out on either a Dec-αA or Silicon Graphics Indigo2 RS10000 workstation, using the Gaussian 94 series

(15) Sheldrick, G. M. *Structure Determination Software Programs*; Siemens X-ray Analytical Instrument Corp., Madison, WI, 1991.

(16) *International Tables For X-ray Crystallography*; Kynoch Press: Birmingham, U.K., 1974; Vol. IV.

(17) Pritzkow, H. Personal communication; Universität Heidelberg, Heidelberg, Germany.

(18) Frisch, M. J.; Trucks, G. W.; Schlegel, H. B.; Gill, P. M. W.; Johnson, B. F. G.; Robb, M. A.; Cheeseman, J. R.; Keith, T.; Peterson, G. A.; Montgomery, J. A.; Raghavachari, K.; Al-Laham, M. A.; Zakrzewski, V. G.; Ortiz, J. V.; Foresman, J. B.; Peng, C. Y.; Ayala, P. Y.; Chen, W.; Wong, M. W.; Andres, J. L.; Replogle, E. S.; Gomperts, R.; Martin, R. L.; Fox, D. J.; Binkley, J. S.; Defrees, D. J.; Baker, J.; Stewart, J. P.; Head-Gordon, M.; Gonzalez, C.; Pople, J. A. *Gaussian 94*, Revisions B.3 & E.2; Gaussian, Inc., Pittsburgh, PA, 1995.

of programs.¹⁸ Most of the calculations were conducted on model compounds in which H's replace the groups exopolyhedrally bound to the cage carbons. Boron-11 NMR chemical shifts of the model compounds were obtained using gauge-independent atomic orbital (GIAO)¹⁹ calculations at the B3LYP/6-311G** level on structures optimized using Becke's three-parameter hybrid methods²⁰ and the correlation functional of Lee, Yang, and Parr²¹ (B3LYP) at the 6-31G* or the 6-311G* levels of theory. Such calculations have been found to give reliable ¹³C and ¹¹B NMR chemical shifts in a number of carbon- and boron-containing compounds.^{22,23} The ¹¹B NMR chemical shifts are relative to the BF₃·OEt₂ standard. In all cases the standard was subjected to the same optimization/GIAO cycle as the particular compound.

Results and Discussion

Syntheses. In most of the syntheses, the C₄B₈ carborane compounds were produced as one of several products in the oxidation of the dilithium compounds of [nido-2-(SiMe₃)-3-(R)-2,3-C₂B₄H₄]²⁻ (R = SiMe₃, n-Bu, t-Bu or Me) by NiCl₂, as shown in Scheme 1. The other products were the corresponding *closo*-1-(SiMe₃)-2-(R)-1,2-C₂B₄H₄ carboranes, as well as nickel metal. The yields of the fusion reactions ranged from a high of 37%, for R = n-Bu (**XI**), to a low of 13%, for R = t-Bu (**VIII**), compared to yields of 69–32% for the corresponding *closo*-carborane products; thus, the C₄B₈ carboranes are minor products in the oxidation reactions. At this point, it is not known whether the two carborane products were produced by competing or consecutive reactions. However, some indirect evidence indicates that the

(19) Wolinski, K.; Hilton, J. F.; Pulay, P. *J. Am. Chem. Soc.* **1990**, *112*, 8251.

(20) Becke, A. D. *J. Chem. Phys.* **1993**, *98*, 5648.

(21) Lee, C.; Yang, W.; Parr, R. G. *Phys. Rev.* **1988**, *B37*, 785.

(22) (a) Ezhova, M. B.; Zhang, H.; Maguire, J. A.; Hosmane, N. S. *J. Organomet. Chem.* **1998**, *550*, 409. (b) Hosmane, N. S.; Lu, K.-J.; Zhang, H.; Maguire, J. A. *Organometallics* **1997**, *16*, 5163.

(23) Cheeseman, J. R.; Trucks, G. W.; Keith, T. A.; Frisch, M. J. *J. Chem. Phys.* **1996**, *104*, 5497.

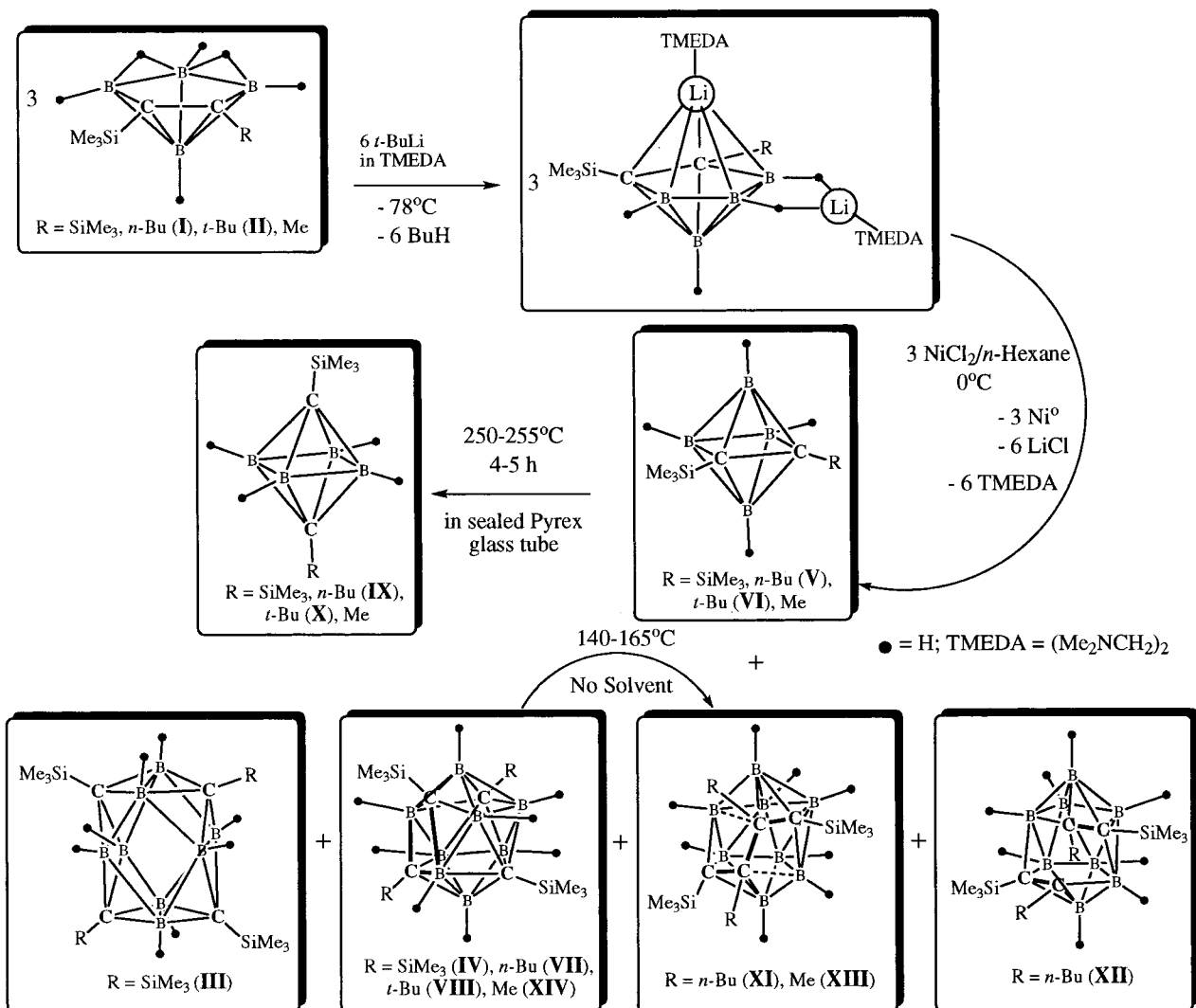
Table 4. Partial Listing of Bond Lengths (Å) and Bond Angles (deg) for III, XI, XII, and XV^a

Bond Lengths (Å)											
Compound III											
C(1)–B(2)	1.672(3)	B(2)–B(3)	1.879(3)	B(3)–B(4)	1.798(3)	B(3)–B(5a)	1.877(3)	B(4)–C(1a)	1.596(3)	B(5)–B(3a)	1.877(3)
C(1)–B(5)	1.685(3)	B(2)–C(6)	1.682(3)	B(3)–C(6)	1.601(3)	B(4)–B(5)	1.893(3)	B(4)–B(2a)	1.904(3)	Si(1)–C(1)	1.866(2)
C(1)–B(3a)	1.604(3)	B(2)–B(4a)	1.904(3)	B(3)–C(1a)	1.604(3)	B(4)–C(6)	1.585(3)	B(5)–C(6)	1.670(3)	Si(2)–C(6)	1.870(2)
C(1)–B(4a)	1.596(3)										
Compound XI											
Si(1)–C(1)	1.892(4)	C(1)–B(7)	1.666(7)	C(3a)–C(4)	1.513(6)	C(4)–B(9)	1.667(7)	B(5)–B(9)	1.796(5)	B(7)–B(8)	1.761(5)
Si(2)–C(4)	1.888(4)	C(2)–B(6)	1.662(7)	C(3a)–B(5)	1.707(7)	B(5)–B(6)	1.829(4)	B(6)–B(7)	1.799(5)	B(8)–B(9)	1.762(5)
C(1)–C(2)	1.516(7)	C(2)–C(11)	1.512(9)	C(3a)–C(11b)	1.550(9)	B(5)–B(8)	1.777(5)	B(6)–B(8)	1.781(5)	B(8)–B(8a)	1.802(7)
C(1)–B(6)	1.700(4)	C(2)–C(3a)	1.508(7)	C(4)–B(5)	1.698(4)						
Compound XII											
Si(1)–C(1)	1.876(8)	B(5)–B(10)	1.887(14)	C(2)–B(7)	1.654(12)	B(7)–B(11)	1.802(14)	C(4)–B(9)	1.735(13)	B(8)–B(12)	1.856(14)
Si(2)–C(3)	1.872(8)	B(5)–B(11)	1.832(14)	C(2)–C(11)	1.526(11)	B(7)–B(12)	1.777(15)	C(4)–B(10)	1.659(13)	B(9)–B(10)	1.797(14)
C(1)–C(2)	1.421(11)	B(6)–B(7)	1.778(15)	C(3)–C(4)	1.415(11)	B(8)–B(9)	1.814(14)	C(4)–C(15)	1.524(12)	B(9)–B(12)	1.730(15)
C(1)–B(5)	1.594(12)	B(6)–B(11)	1.738(15)	C(3)–B(8)	1.596(14)	C(3)–B(9)	1.669(13)	B(5)–B(6)	1.830(15)	B(10)–B(11)	1.757(15)
C(1)–B(6)	1.683(14)	C(2)–B(6)	1.741(13)	B(7)–B(8)	1.884(14)						
Compound XV											
Br–B(14)	1.920(6)	C(11)–B(15)	1.692(5)	B(12)–B(16)	1.797(5)	C(13)–B(17)	1.801(4)	B(15)–B(16)	1.717(6)	B(16)–B(17)	1.888(6)
Si(1)–C(11)	1.885(5)	B(12)–C(13)	1.666(6)	C(13)–B(14)	1.521(4)	C(13)–C(21)	1.525(5)	B(15)–C(18)	1.745(6)	B(16)–C(18)	1.687(4)
Si(2)–C(18)	1.902(4)	B(12)–B(15)	1.762(6)	C(13)–B(16)	1.680(5)	B(14)–B(17)	1.948(7)	B(15)–B(15a)	1.751(8)	B(17)–C(18)	1.787(8)
C(11)–B(12)	1.642(5)										
Bond Angles (deg)											
Compound III											
B(2)–C(1)–B(5)	81.6(1)	B(3)–B(4)–B(5)	95.6(1)	C(6)–B(2)–B(4a)	127.1(2)	C(1)–B(5)–C(6)	96.6(1)				
B(2)–C(1)–B(3a)	113.4(2)	B(3)–B(4)–C(6)	56.1(1)	B(2)–B(3)–B(4)	96.4(1)	B(4)–B(5)–C(6)	52.4(1)				
B(5)–C(1)–B(3a)	69.5(1)	B(5)–B(4)–C(6)	56.5(1)	B(2)–B(3)–C(6)	57.1(1)	C(1)–B(5)–B(3a)	53.2(1)				
B(2)–C(1)–B(4a)	71.2(1)	B(3)–B(4)–C(1a)	56.0(1)	B(4)–B(3)–C(6)	55.2(1)	B(4)–B(5)–B(3a)	109.2(1)				
B(5)–C(1)–B(4a)	113.5(2)	B(5)–B(4)–C(1a)	111.6(1)	B(2)–B(3)–C(1a)	112.6(2)	C(6)–B(5)–B(3a)	127.9(1)				
B(3a)–C(1)–B(4a)	68.4(1)	C(6)–B(4)–C(1a)	108.2(2)	B(4)–B(3)–C(1a)	55.6(1)	B(2)–C(6)–B(4)	114.1(1)				
C(1)–B(2)–B(3)	127.7(2)	B(3)–B(4)–B(2a)	95.4(1)	C(6)–B(3)–C(1a)	107.0(2)	B(3)–C(6)–B(4)	68.7(1)				
C(1)–B(2)–C(6)	96.6(1)	B(5)–B(4)–B(2a)	69.4(1)	B(2)–B(3)–B(5a)	70.2(1)	B(2)–C(6)–B(5)	81.7(1)				
B(3)–B(2)–C(6)	53.1(1)	C(6)–B(4)–B(2a)	111.7(1)	B(4)–B(3)–B(5a)	96.6(1)	B(3)–C(6)–B(5)	113.4(1)				
C(1)–B(2)–B(4a)	52.5(1)	C(1a)–B(4)–B(2a)	56.2(1)	C(6)–B(3)–B(5a)	112.4(2)	B(4)–C(6)–B(5)	71.1(1)				
B(3)–B(2)–B(4a)	108.6(1)	C(1)–B(5)–B(4)	127.6(1)	C(1a)–B(3)–B(5a)	57.2(1)						
Compound XI											
C(2)–C(1)–B(6)	61.9(3)	C(2)–B(6)–B(8)	117.1(3)	C(4)–B(5)–B(6)	117.9(2)	B(6)–B(8)–B(9)	111.3(3)				
C(2)–C(1)–B(7)	113.3(3)	B(5)–B(6)–B(8)	59.0(2)	C(4)–B(5)–B(8)	109.1(3)	B(7)–B(8)–B(9)	111.4(3)				
B(6)–C(1)–B(7)	64.6(2)	B(7)–B(6)–B(8)	58.9(2)	B(6)–B(5)–B(8)	59.2(2)	B(5)–B(8)–B(8a)	105.2(2)				
C(2)–C(1)–B(6a)	96.4(3)	C(1)–B(7)–B(6)	58.6(2)	C(4)–B(5)–B(9)	56.9(2)	B(6)–B(8)–B(8a)	105.1(2)				
B(6)–C(1)–B(6a)	106.8(3)	C(1)–B(7)–B(8)	111.7(3)	B(6)–B(5)–B(9)	107.6(3)	B(7)–B(8)–B(8a)	59.2(1)				
B(7)–C(1)–B(6a)	64.6(2)	B(6)–B(7)–B(8)	60.0(2)	B(8)–B(5)–B(9)	59.1(2)	B(9)–B(8)–B(8a)	59.2(1)				
C(1)–C(2)–B(6)	64.5(3)	B(6)–B(7)–B(6a)	98.7(4)	C(1)–B(6)–C(2)	53.6(3)	C(4)–B(9)–B(5)	58.6(2)				
C(1)–C(2)–C(11)	121.6(4)	B(8)–B(7)–B(6a)	106.0(3)	C(1)–B(6)–B(5)	118.8(3)	C(4)–B(9)–B(8)	111.3(3)				
B(6)–C(2)–C(11)	114.4(4)	B(8)–B(7)–B(8a)	61.5(3)	C(2)–B(6)–B(5)	78.1(2)	B(5)–B(9)–B(8)	59.9(2)				
C(1)–C(2)–C(3a)	107.9(4)	B(5)–B(8)–B(6)	61.9(2)	C(1)–B(6)–B(7)	56.8(2)	B(5)–B(9)–B(5a)	99.1(3)				
B(6)–C(2)–C(3a)	119.4(4)	B(5)–B(8)–B(7)	111.5(3)	C(2)–B(6)–B(7)	100.3(3)	B(8)–B(9)–B(5a)	106.1(3)				
C(11)–C(2)–C(3a)	118.1(5)	B(6)–B(8)–B(7)	61.1(2)	B(5)–B(6)–B(7)	107.4(2)	C(4)–B(9)–B(8a)	111.3(3)				
B(5)–C(4)–B(9)	64.5(2)	B(5)–B(8)–B(9)	61.0(2)	C(1)–B(6)–B(8)	109.1(3)	B(8)–B(9)–B(8a)	61.5(3)				
B(5)–C(4)–C(3a)	94.7(3)	B(5)–C(4)–B(5a)	107.2(3)								
Compound XII											
C(2)–C(1)–B(5)	110.0(7)	C(2)–B(7)–B(12)	121.0(7)	C(1)–B(5)–B(6)	58.4(5)	C(4)–B(10)–B(12)	104.4(7)				
C(2)–C(1)–B(6)	67.6(6)	B(6)–B(7)–B(12)	114.3(7)	C(1)–B(5)–B(10)	127.1(7)	B(5)–B(10)–B(12)	104.6(7)				
B(5)–C(1)–B(6)	67.9(6)	B(8)–B(7)–B(12)	60.9(6)	B(6)–B(5)–B(10)	108.7(7)	B(9)–B(10)–B(12)	57.3(6)				
C(1)–C(2)–B(6)	63.4(6)	B(11)–B(7)–B(12)	59.3(6)	C(1)–B(5)–B(11)	107.3(7)	B(11)–B(10)–B(12)	59.4(6)				
C(1)–C(2)–B(7)	115.8(7)	C(3)–B(8)–B(7)	127.7(7)	B(6)–B(5)–B(11)	56.7(6)	B(5)–B(11)–B(6)	61.6(6)				
B(6)–C(2)–B(7)	63.1(6)	C(3)–B(8)–B(9)	58.2(6)	B(10)–B(5)–B(11)	56.3(5)	B(5)–B(11)–B(7)	97.2(6)				
B(7)–C(2)–C(11)	116.7(7)	B(7)–B(8)–B(9)	108.7(7)	C(1)–B(6)–C(2)	49.0(5)	B(6)–B(11)–B(7)	60.3(6)				
C(4)–C(3)–B(8)	110.0(7)	C(3)–B(8)–B(12)	107.1(7)	C(1)–B(6)–B(5)	53.7(5)	B(5)–B(11)–B(10)	63.4(6)				
C(4)–C(3)–B(9)	67.9(6)	B(7)–B(8)–B(12)	56.7(5)	C(2)–B(6)–B(5)	87.6(6)	B(6)–B(11)–B(10)	119.7(8)				
B(8)–C(3)–B(9)	67.4(6)	B(9)–B(8)–B(12)	56.2(6)	C(1)–B(6)–B(7)	97.8(7)	B(7)–B(11)–B(10)	105.4(7)				
C(3)–C(4)–B(9)	63.0(5)	C(3)–B(9)–C(4)	49.1(5)	C(2)–B(6)–B(7)	56.1(5)	B(5)–B(11)–B(12)	108.8(7)				
C(3)–C(4)–B(10)	116.3(7)	C(3)–B(9)–B(8)	54.4(5)	B(5)–B(6)–B(7)	98.1(7)	B(6)–B(11)–B(12)	116.7(7)				
B(9)–C(4)–B(10)	63.9(6)	C(4)–B(9)–B(8)	88.2(6)	C(1)–B(6)–B(11)	107.6(7)	B(7)–B(11)–B(12)	59.6(6)				
C(2)–B(6)–B(11)	103.5(7)	C(3)–B(9)–B(10)	97.9(7)	B(8)–B(9)–B(12)	63.1(6)	B(10)–B(11)–B(12)	61.9(6)				
B(5)–B(6)–B(11)	61.7(6)	C(4)–B(9)–B(10)	56.0(5)	B(10)–B(9)–B(12)	61.8(6)	B(7)–B(12)–B(8)	62.4(6)				
B(7)–B(6)–B(11)	61.7(6)	B(8)–B(9)–B(10)	98.4(7)	C(4)–B(10)–B(5)	73.6(6)	B(7)–B(12)–B(9)	117.9(7)				
C(2)–B(7)–B(6)	60.8(5)	C(3)–B(9)–B(12)	109.8(7)	C(4)–B(10)–B(9)	60.1(5)	B(8)–B(12)–B(9)	60.6(6)				
C(2)–B(7)–B(8)	72.3(6)	C(4)–B(9)–B(12)	104.8(7)	B(5)–B(10)–B(9)	119.1(7)	B(7)–B(12)–B(10)	104.2(7)				
B(6)–B(7)–B(8)	119.5(7)	B(9)–B(12)–B(10)	60.9(6)	C(4)–B(10)–B(11)	121.1(7)	B(8)–B(12)–B(10)	96.3(7)				
C(2)–B(7)–B(11)	104.4(7)	B(7)–B(12)–B(11)	61.1(6)	B(5)–B(10)–B(11)	60.2(6)	B(9)–B(12)–B(11)	115.7(8)				
B(6)–B(7)–B(11)	58.1(6)	B(8)–B(12)–B(11)	106.6(7)	B(9)–B(10)–B(11)	113.0(7)	B(10)–B(12)–B(11)	58.7(6)				
B(8)–B(7)–B(11)	104.2(7)										

Table 4. (Continued)

Bond Angles (deg) (continued)					
Compound XV					
B(12)–C(11)–B(15)	63.8(2)	B(14)–C(13)–B(17)	71.3(2)	B(12)–B(15)–B(16)	62.2(2)
B(12)–C(11)–B(12a)	116.5(5)	B(16)–C(13)–B(17)	65.6(2)	C(11)–B(15)–C(18)	100.7(3)
B(12)–C(11)–B(15a)	116.0(3)	Br–B(14)–C(13)	121.6(2)	B(12)–B(15)–C(18)	103.7(3)
B(15)–C(11)–B(15a)	62.4(3)	Br–B(14)–B(17)	147.1(4)	B(16)–B(15)–C(18)	58.3(2)
C(11)–B(12)–C(13)	117.7(3)	C(13)–B(14)–B(17)	61.1(2)	C(11)–B(15)–B(15a)	58.8(1)
C(11)–B(12)–B(15)	59.5(2)	C(13)–B(14)–C(13a)	115.9(4)	B(12)–B(15)–B(15a)	107.2(2)
C(13)–B(12)–B(15)	110.3(3)	C(11)–B(15)–B(12)	56.7(2)	B(16)–B(15)–B(15a)	110.5(2)
C(11)–B(12)–B(16)	104.7(3)	C(11)–B(15)–B(16)	106.1(3)	C(18)–B(15)–B(15a)	59.9(2)
C(13)–B(12)–B(16)	57.9(2)	B(14)–B(17)–C(18)	123.3(4)	B(12)–B(16)–C(13)	57.2(2)
B(15)–B(12)–B(16)	57.7(2)	B(16)–B(17)–C(18)	54.6(2)	B(12)–B(16)–B(15)	60.2(2)
B(12)–C(13)–B(14)	103.5(3)	C(13)–B(17)–C(13a)	91.4(3)	C(13)–B(16)–B(15)	111.9(3)
B(12)–C(13)–B(16)	64.9(2)	C(13)–B(17)–B(16a)	122.3(3)	B(12)–B(16)–B(17)	97.8(3)
B(14)–C(13)–B(16)	128.3(3)	B(16)–B(17)–B(16a)	103.0(4)	C(13)–B(16)–B(17)	60.3(2)
B(12)–C(13)–B(17)	106.4(3)	B(15)–C(18)–B(16)	60.0(2)	B(15)–B(16)–B(17)	106.8(3)
				B(12)–B(16)–C(18)	104.6(3)
				C(13)–B(16)–C(18)	112.4(3)
				B(15)–B(16)–C(18)	61.7(3)
				B(17)–B(16)–C(18)	59.7(3)
				C(13)–B(17)–B(14)	47.7(2)
				C(13)–B(17)–B(16)	54.1(2)
				B(14)–B(17)–B(16)	97.4(2)
				C(13)–B(17)–C(18)	102.5(3)
				B(15)–C(18)–B(17)	110.2(3)
				B(16)–C(18)–B(17)	65.8(2)
				B(15)–C(18)–B(15a)	60.3(3)
				B(16)–C(18)–B(15a)	112.3(3)
				B(16)–C(18)–B(16a)	122.3(4)

^a Bond distances and bond angles for **IV** can be found in the Supporting Material.

Scheme 1. Syntheses of *closo*-C₂B₄ and *nido*-C₄B₈ Carboranes

former is most likely the case. There was no hint of interconversion between the *closo* and the fusion products when either was heated for prolonged periods of time in the presence of NiCl₂ and/or finely divided nickel metal. In addition, while many of the fusion products were thermally unstable, they did not decompose to the *closo* compounds. There were four different cage-atom arrangements found in the fusion products, examples of each are shown in Figures 1–5. Depending on the

relative positions of the cage carbon atoms, the structures can be grouped into the “carbons apart” cages **III**, **IV**, and **XV**, in which the cage carbons are separated by at least one boron atom, as shown in Figures 1, 2 and 5, respectively, and the “carbons adjacent” cages, **XI** and **XII**, in which at least two of the cage carbons are within normal bonding distances (see Figures 3 and 4, respectively). The nature of the starting *nido*-carboranes dictates the type of fusion product formed;

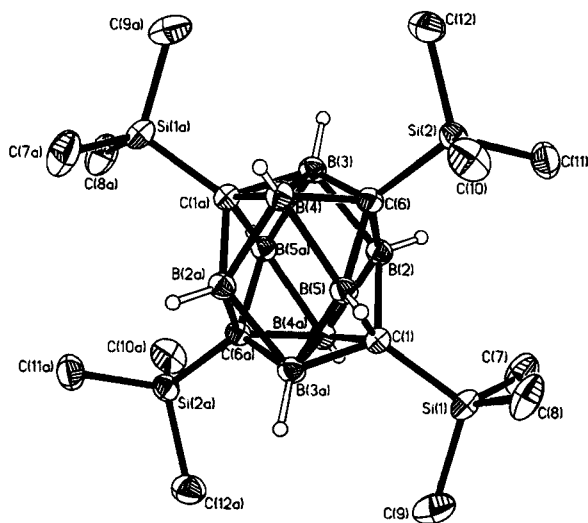


Figure 1. Crystal structure of the "carbons apart" tetracarbon carborane *nido*-2,4,7,9-(SiMe₃)₄-2,4,7,9-C₄B₈H₈ (**III**), showing the atom-numbering scheme. The thermal ellipsoids are drawn at the 40% probability level. For clarity, the H atoms of the SiMe₃ groups are omitted.

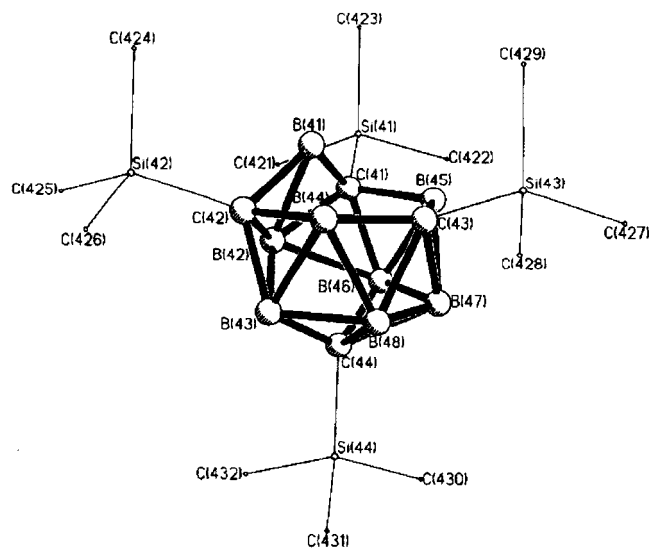


Figure 2. Perspective view of one of the crystallographically independent molecules of the "carbons apart" tetracarbon carborane *nido*-2,4,6,12-(SiMe₃)₄-2,4,6,12-C₄B₈H₈ (**IV**), showing the atom-numbering scheme. For clarity, the H atoms of the cage are omitted and the cage-bound SiMe₃ groups are drawn with circles of arbitrary radii.

the TMEDA-solvated dilithium compound of the bis(trimethylsilyl)-substituted carborane dianion [*nido*-2,3-(SiMe₃)₂-2,3-C₂B₄H₄]²⁻ produced the "carbons apart" isomers **III** and **VI**, while the "carbons adjacent" compounds **XI** and **XII** were obtained when the *n*-Bu/SiMe₃-substituted carborane monoanion [2-(SiMe₃)-3-(*n*-Bu)-2,3-C₂B₄H₅]⁻ was used. The synthetic routes to the two types of fusion products are not exclusive; a small amount (12% yield) of a "carbons adjacent" compound, **XIII**, was obtained from the oxidation of [2-(SiMe₃)-3-(Me)-2,3-C₂B₄H₄]²⁻ by NiCl₂, while the "carbons apart" compound **VIII** was obtained in 18% yield from the oxidation of the monoanion [2-(SiMe₃)-3-(*n*-Bu)-2,3-C₂B₄H₅]⁻. It is of interest to note that no *closo*-carborane coproduct was found in the oxidation of the

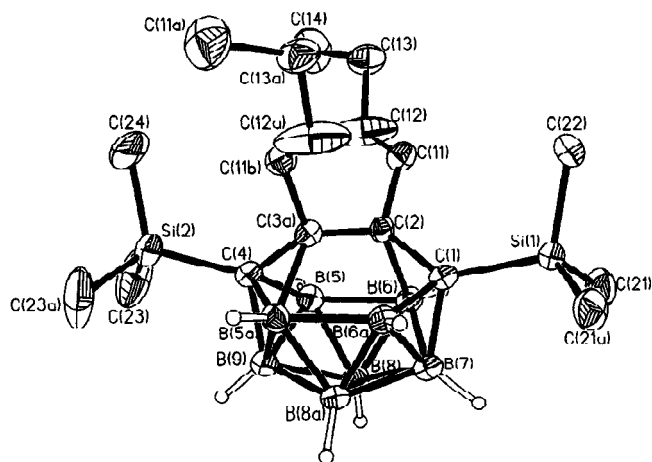


Figure 3. Crystal structure of the "carbons adjacent" tetracarbon carborane *nido*-1,4-(SiMe₃)₂-2,3-(*n*-Bu)₂-1,2,3,4-C₄B₈H₈ (**XI**), showing the atom-numbering scheme. The thermal ellipsoids are drawn at the 40% probability level. For clarity, the H atoms of the trimethylsilyl and *n*-butyl groups are omitted.

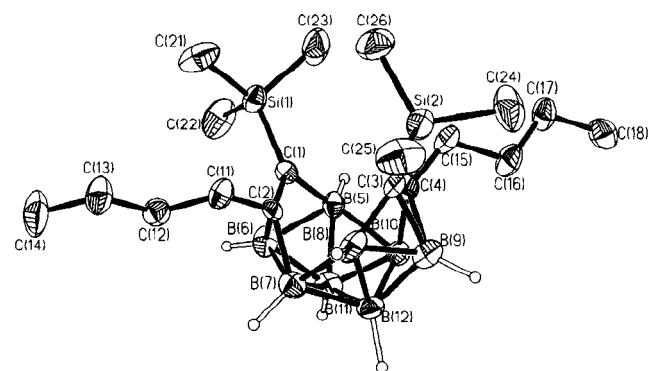


Figure 4. Crystal structure of the "carbons adjacent" tetracarbon carborane *nido*-2,8-(SiMe₃)₂-3,9-(*n*-Bu)₂-2,3,8,9-C₄B₈H₈ (**XII**), showing the atom-numbering scheme. The thermal ellipsoids are drawn at the 40% probability level. For clarity, the H atoms of the trimethylsilyl and *n*-butyl groups are omitted.

monoanion; the other product in that reaction was the neutral *nido*-carborane **I**, formed in 38% yield.

Compound **III**, which has been described in a preliminary report,¹⁰ is unusual in that its structure is based more on the cuboctahedron than the icosahedron (see Figure 1). While **III** is air-stable, it isomerizes at moderate temperatures (100 °C) to give **IV**. Both isomers are characterized by the fact that there are no adjacent cage carbons: hence, the "carbons apart" designation. These two compounds were isolated in essentially equimolar quantities from the reaction of the bis(trimethylsilyl)carborane dianion [*nido*-2,3-(SiMe₃)₂-2,3-C₂B₄H₄]²⁻ and NiCl₂. However, since the isolation of **III** and **IV** required extended heating at 100–120 °C, which is above or at the optimum temperature for the conversion of **III** to **IV** (100 °C), little significance can be placed in the observation of a 1:1 product ratio. The results are more consistent with a sequence in which **III** is the initially formed fusion product, which is partially converted to **IV** during workup. In this regard, it should be noted that the isolation and purification procedures used in the syntheses of **VII** and **VIII**, which

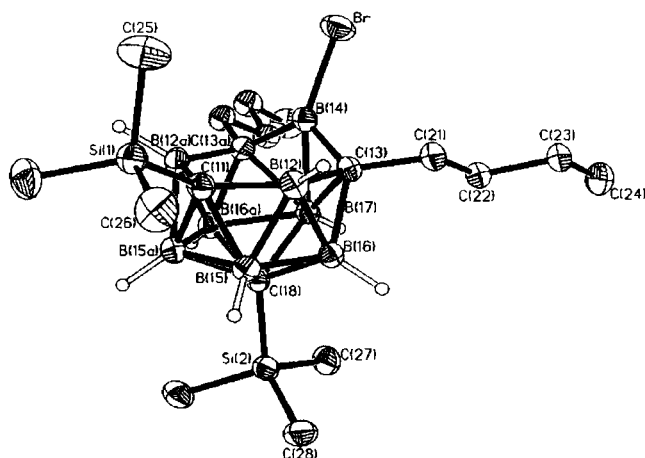


Figure 5. Crystal structure of the “carbons apart” tetra-carbon carborane *nido*-1-Br-2,6-(*n*-Bu)₂-4,12-(SiMe₃)₂-2,4,6,12-C₄B₈H₈ (**XV**), showing the atom-numbering scheme. The thermal ellipsoids are drawn at the 40% probability level. For clarity, the H atoms of the trimethylsilyl and *n*-butyl groups are omitted.

are analogues of **IV**, required prolonged heating at temperatures in excess of 100 °C; under these conditions, only the more thermally stable isomers, with structures similar to **IV**, would be isolated. As pointed out above, the “carbons adjacent” C₄B₈ cages (**XI–XIII**) could only be obtained from the oxidative fusion reactions of the monoanion of **I**, [*nido*-2-(SiMe₃)₂-3-(*n*-Bu)-2,3-C₂B₄H₅][−], or the less sterically hindered [*nido*-2-(SiMe₃)₂-3-(Me)-2,3-C₂B₄H₄]^{2−}. The cage structures of **XI** and **XII** are essentially those reported by Grimes for (CH₃)₄C₄B₈H₈ and (C₂H₅)₄C₄B₈H₈, respectively.^{4,5} This is not too surprising, since the synthesis of **XI** is similar to that used by Grimes in that both involve the reaction of the monoanion of a *nido*-2,3-C₂B₄ carborane with an easily reduced divalent transition-metal halide. In Grimes' syntheses FeCl₂ was used, followed by air oxidation,² while for **XI** and **XII**, the more easily reduced NiCl₂ was used^{24,25} and no additional oxidant was needed. Since an outside oxidant was required when FeCl₂ was used, the intermediate metallacarborane [2,3-(CH₃)₂-2,3-C₂B₄H₄]₂FeH₂ could be isolated and structurally characterized.²⁶ The structure showed that the Fe was sandwiched between two [2,3-(CH₃)₂-2,3-C₂B₄H₄]^{2−} ligands oriented such that the cage carbons on the opposing carboranes were almost eclipsed, with a cage carbon atom on one carborane being situated almost directly over one in the other ligand. Although the metal-bound hydrogens could not be located, it was speculated that they occupied bridging positions on the FeB₂ polyhedral faces and that such bridging promoted the almost eclipsed positions of the cage carbons. The authors rationalized the structure of their C₄B₈ fusion products on the basis that the intermediate ferracarboranes serve as templates in directing a contiguous grouping of the cage carbons to give “carbons adjacent” compounds. Following that reasoning, it is quite plausible to assume that the fusion products in the present study (**III**, **IV**, **VII**, **VIII**, **XI–XIV**) arise from the

disproportionation of intermediate nickelacarborane sandwich complexes and that the geometries of those intermediates dictate the structures of the fusion products. The NiCl₂-mediated addition of Me₂C₂ to [2,3-Et₂C₂B₄H₅][−] to give 4,5,7,8-Me₂Et₂C₄B₄H₄ studied by Mirabelli and Sneddon is also thought to go through an intermediate nickelacarborane of the form 1-(Me₂C₂)-1-Ni-2,3-Et₂C₂B₄H₄, which decomposes to give the tetra-carbon carborane and nickel metal.²⁷ While it was not possible to isolate an intermediate nickelacarborane, a number of related metallacarboranes have been synthesized and their structures determined. The structures of the chromacarboranes [*commo*-1,1'-Cr{2,3-(SiMe₃)₂-1,2,3-CrC₂B₄H₄]₂^{*n*−} (*n* = 0, 1) have been determined and show that the Cr atoms are sandwiched between two equivalent carborane cages that are oriented so that the cage carbons occupy trans positions across the metal center.¹⁴ It is significant that the chromacarboranes with these orientations produce only the “carbons apart” fusion product **IV**. Trans orientations of the cage carbons have also been observed in the related icosahedral complexes [M(1,2-C₂B₉H₁₁)₂]^{*n*−} (*n* = 2, M = Ni, Pd; *n* = 1, M = Ni).²⁸ On the other hand, [M(1,2-C₂B₉H₁₁)₂]^{*n*−} (*n* = 0, M = Ni;²⁹ *n* = 1, M = Co³⁰) complexes show a nearly eclipsed (cisoid) orientation in which the cage carbons on opposing carborane ligands are on the same side of the metallacarborane. Cis orientations were also found in the full-sandwich zircona- and titanacarboranes in the C₂B₄ cage system.^{31,32} Unfortunately, it is not presently possible to predict the orientation of the cage carbons in the full-sandwich metallacarboranes; while the presence of bridging groups, either H's²⁶ or metal groups,^{31,32} may promote eclipsed arrangements, they are not a necessary structural feature.^{29–32} Compounds **XI** and **XII** are products of the reaction of the [2-(SiMe₃)₂-3-(*n*-Bu)-2,3-C₂B₄H₅][−] monoanion with NiCl₂, and the possibility exists for the formation of a diprotonated intermediate nickelacarborane with a structure similar to that of [2,3-(CH₃)₂-2,3-C₂B₄H₄]₂FeH₂. Decomposition of such a metallacarborane would naturally lead to the formation of “carbon adjacent” C₄B₈ fusion products, such as **XI–XIII**. It is difficult to visualize how the “carbons apart” C₄B₈ clusters (**III**, **IV**, **VII**, **VIII**, and **XIV**) could arise from an eclipsed metallacarborane precursor. On the other hand, compound **III** would be formed directly from the oxidative fusion of two metal-bound carborane cages whose cage carbons were oriented in a trans configuration across a metal center, similar to that found for the chromacarboranes; **IV** could arise from the thermal isomerization of **III**. In the same way, compounds analogous to **III** could be the initially formed kinetic products in all the “carbons apart” fusion syntheses and

(27) Mirabelli, M. G. L.; Sneddon, L. G. *Organometallics* **1986**, *5*, 1510.

(28) Warren, L. F., Jr.; Hawthorne, M. F. *J. Am. Chem. Soc.* **1970**, *92*, 1157.

(29) St. Clair, D.; Zalkin, A.; Templeton, D. H. *J. Am. Chem. Soc.* **1970**, *92*, 1173.

(30) (a) Zalkin, A.; Hopkins, T. E.; Templeton, D. H. *Inorg. Chem.* **1967**, *6*, 1911. (b) Borodinsky, L.; Sinn, E.; Grimes, R. N. *Inorg. Chem.* **1982**, *21*, 1686.

(31) Thomas, C. J.; Jia, L.; Zhang, H.; Siriwardane, U.; Maguire, J. A.; Wang, Y.; Brooks, K. A.; Weiss, V. P.; Hosmane, N. S. *Organometallics* **1995**, *14*, 1365.

(32) Hosmane, N. S.; Wang, Y.; Zhang, H.; Lu, K.-J.; Maguire, J. A.; Gray, T. G.; Brooks, K. A.; Waldh r, E.; Kaim, W.; Kremer, R. K. *Organometallics* **1997**, *16*, 1365.

(24) The standard reduction of Ni²⁺ is −0.250 V, compared to −0.440 V for Fe²⁺ (see ref 24).

(25) Milazzo, G.; Caroli, S.; Sharma, V. K. *Tables of Standard Electrode Potentials*; Wiley: London, 1978.

(26) Pipal, J. R.; Grimes, R. N. *Inorg. Chem.* **1979**, *18*, 263.

would thermally rearrange to **VII**, **VIII**, and **XIV** during workup. In this regard, one would expect that bulky groups, such as SiMe₃ and *t*-Bu, would favor the formation of trans-oriented metallacarborane intermediates and that replacement of an SiMe₃ group with a less sterically demanding *n*-Bu or Me could allow the formation of a metallacarborane with eclipsed cage carbons, affording "carbons adjacent" fusion products. This is what is found experimentally. Therefore, we propose a mechanism for the cage fusion reactions that involves the initial formation of a full-sandwich nickelacarborane that disproportionates to give the fusion products; the relative positions of the cage carbons in this intermediate will determine whether "carbons apart" or "carbons adjacent" carboranes dominate the products.

Structures. The structures of compounds **III**, **IV**, **XI**, **XII**, and **XV** were determined by single-crystal X-ray diffraction studies and are shown in Figures 1–5, respectively. Selected bond lengths and bond angles of **III**, **XI**, **XII**, and **XV** are given in Table 4. A more complete listing of bond lengths and bond angles, as well as those for **IV**, are included in the Supporting Information. The structures of the other C₄B₈ fusion products (**VII**, **VIII**, **XIII**, and **XIV**) were inferred from the similarities of their ¹¹B and ¹³C NMR spectra to those of one of the structurally characterized carboranes. The solution NMR spectra of all the compounds show nonrigid stereochemistry, leading to fluxionality or rapid isomerization; the problems encountered in solving the solid-state structure of **IV** could also reflect this nonrigidity.

As pointed out above, the structure of **III** is unusual in that it possesses a 12-vertex cage of D_{2h} symmetry that is derived from the distortion of a cuboctahedron rather than an icosahedron (see Figure 1). The distortions are such that unequal B–B distances are found in the molecule; the shortest distances (1.798(3) Å) are between B(3) and B(4), while the next shortest are those on the B₄ faces (B(2)–B(3)–B(5a)–B(4a)), which average 1.889 ± 0.011 Å.³³ These are comparable to the B_{apical}–B_{basal} distance of 1.795 ± 0.006 Å in the precursor dianion.⁷ The B(2)–B(5), B(2a)–B(5), and B(3a)–B(4) distances in **III** are much larger, being 2.192, 2.161, and 3.072 Å, respectively. Some caution must be exercised in viewing Figure 1 in that connectivity lines are shown between the cage atoms when their internuclear distances are less than 2 Å. For example, even though they are not connected, there is probably significant interaction between B(5) and B(2) or B(2a). Table 5 lists some interatomic distances found in the B3LYP/6-31G*-optimized structure of the model compound C₄B₈H₁₂ (**III'**), in which H's replace the SiMe₃ groups on the cage carbons of **III**. The optimized geometry of the model compound has D_{2h} symmetry, with a cage quite similar to that shown in Figure 1; a comparison of the equivalent distances in the two structures shows very little differences. Therefore, any effects of the SiMe₃ groups on the structure of **III** are probably quite small. Specifically, the distortion from the D_{4h} symmetry of a cuboctahedral structure is not due to the presence of the SiMe₃ groups.

While the structure of **III** is well-defined, that of **IV**, the thermodynamically more stable "carbons apart"

Table 5. Interatomic Distances (Å) Calculated for Model Compounds **III'**, **IV'**, **XI'**, **XII'**, and **XV'**^{a,b}

Compound III'					
C(1)–B(2)	1.684	C(6)–B(3)	1.589	C(1)–C(6)	2.483
B(2)–B(3)	1.906	B(2)–B(5)	2.230	B(3)–B(4)	1.820
B(5)–B(2a)	2.050	B(4)–B(3a)	3.188		
Compound IV'					
C(1)–B(1)	1.529	C(3)–B(8)	1.700	B(1)–B(4)	2.621
C(1)–B(2)	1.792	C(3)–B(5)	1.634	B(2)–B(3)	1.906
C(1)–B(5)	1.661	C(4)–B(6)	1.688	B(3)–B(8)	1.714
C(1)–B(6)	1.659	C(4)–B(7)	1.737	B(3)–B(4)	1.787
C(3)–B(4)	1.634	B(1)–B(2)	1.912	B(4)–B(8)	1.773
				B(7)–B(8)	1.775
Compound XI'					
C(1)–C(2)	1.483	C(3a)–B(5)	2.400	B(5)–B(9)	1.822
C(1)–B(6)	1.725	C(4)–B(5)	1.661	B(6)–B(8)	1.795
C(1)–B(7)	1.668	B(5)–B(6)	1.850	B(7)–B(8)	1.781
C(2)–B(6)	1.671	B(5)–B(8)	1.762	B(8)–B(8a)	1.826
C(2)–C(3a)	1.511				
Compound XII'					
C(1)–C(2)	1.411	C(4)–B(9)	1.741	B(7)–B(11)	1.823
C(1)–B(5)	1.563	C(4)–B(10)	1.622	B(7)–B(12)	1.781
C(1)–B(6)	1.660	B(5)–B(6)	1.870	B(10)–B(12)	1.820
C(2)–B(6)	1.740	B(5)–B(10)	1.891	B(8)–B(9)	1.867
C(2)–B(7)	1.618	B(5)–B(11)	1.860	B(8)–B(12)	1.851
C(3)–C(4)	1.416	B(6)–B(7)	1.817	B(9)–B(10)	1.810
C(3)–B(8)	1.558	B(6)–B(11)	1.734	B(9)–B(12)	1.738
C(3)–B(9)	1.658	B(7)–B(8)	1.898	B(10)–B(11)	1.776
Compound XV'					
Br–B(1)	1.935	C(3)–B(4)	1.522	B(5)–C(8)	1.738
C(1)–B(1)	1.634	C(3)–B(6)	1.666	B(5)–B(5a)	1.777
C(1)–B(5)	1.698	C(3)–B(7)	1.809	B(6)–B(7)	1.896
B(2)–C(3)	1.656	B(4)–B(7)	1.941	B(6)–C(8)	1.685
B(2)–B(5)	1.771	B(5)–B(6)	1.715	B(7)–C(8)	1.734
B(2)–B(6)	1.789				

^a Optimized at the B3LYP/6-31G* level for **III'**, **IV'**, **XI'**, and **XII'** and at the B3LYP/6-311G** level for **XV'**. ^b The atom numbering system is same as in the respective unprimed molecules (**III**, **IV**, **XI**, **XII**, and **XV**).

isomer, is not. Single-crystal X-ray diffraction analysis of **IV** resulted in a structure containing six crystallographically independent molecules in the unit cell of the compound; one of the six molecules is shown in Figure 2. This structure shows a more open cage having one six-membered, nonplanar open face (B(41)–C(41)–B(45)–C(43)–B(44)–C(42)) and a smaller four-membered face (B(42)–B(46)–C(44)–B(43)). However, the B(42)–B(46) and B(42)–B(43) distances are in the outer range of normal B–B bonding distances. If one assumes that they are not bonded, the cage would have two six-membered open faces. An analysis of the different structures in the unit cell of **IV** shows that the main differences among the molecules are in the positions of the B(41) and B(42) atoms relative to the other cage atoms. Since **IV** is the more stable isomer and the one most often produced by the synthetic methods used, a number of attempts were made to clarify its structure. Since multiple recrystallizations and syntheses, as well as X-ray diffraction studies at lower temperatures (–110 °C), gave the same results,¹⁷ compound **XV**, a boron-brominated derivative of **IV**, was prepared and its structure determined (see Figure 5). In addition, the structures of the model compounds **IV'** and **XV'** were optimized at the B3LYP/6-31G* and B3LYP/6-311G* levels, respectively, and the results are summarized in Table 5. As with **III'**, these model compounds were the

(33) Whenever the average value of a parameter is given, the indetermination listed is the average deviation.

same as the bis(trimethylsilyl)-substituted derivatives except that H's replace the SiMe₃'s on the cage carbons. A comparison of the equivalent internuclear distances in **XV** with its model compound (**XV'**) shows that they agree to within ± 0.011 Å; a comparison of analogous distances of the cage atoms in **IV'** and **XV'** shows similar agreement. Figure 5 shows that the cage of **XV** possesses C_s symmetry with a mirror plane containing the Br, B(14), B(17), and C(18) atoms; the cluster has a nonplanar C₃B₃ six-membered open face (B(14)–C(13)–B(12)–C(11)–B(12a)–C(13a)) situated above a five-membered ring of boron atoms (B(17)–B(16)–B(15)–B(15a)–B(16a)) that are bonded to an apical carbon atom, C(18) (see Figure 5). At least formally, the structures of **IV** and **XV** are similar to those of the nido-[(CR)₂B₁₀H₁₀]²⁻ cages found in the MC₂B₁₀ metallacarboranes.^{34,35} Both have open six-membered faces surmounting five-membered rings of boron atoms that are bonded to an apical atom; in the MC₂B₁₀ system the apical atoms are borons, while in **IV** and **XV** they are carbons. This similarity in cage structure is not surprising, since both the C₄B₈ and the [C₂B₁₀]²⁻ cages are 12-vertex clusters with 28 cage electrons (*n* + 2 pairs), which should give rise to a nido structure. While the cage of **XV** can be classified as nido, it is very distorted. The six-membered face is nonplanar, with B(14) being significantly displaced above the plane of the other five facial atoms; the dihedral angle between the planes defined by the C(13)–B(12)–C(11)–B(12a)–C(13a) and the C(13)–B(14)–C(13a) atoms is 68°. This could be the result of the heteroatomic nature of the face; however, a similar nonplanarity is also seen in the lower five-membered ring, but to a much smaller extent. The dihedral angle between the B(16)–B(15)–B(15a)–B(16a) and B(16)–B(17)–B(16a) planes is 15°. In addition, the apical carbon, C(18) in Figure 5, is not symmetrically bound to the five boron atoms in the lower ring, in that the C(18)–B(16) distance of 1.687 Å is significantly shorter than the C(18)–B(17) and C(18)–B(15) distances of 1.787 and 1.745 Å, respectively. Since the calculated bond distances in **XV'** are 1.685, 1.734, and 1.738 Å, respectively (see Table 5), which are quite similar to those found in **XV**, these variations reflect a difference in intracage bonding preferences rather than experimental indetermination or the presence of different cage-carbon substituents. In general, the C_{cage}–B and B–B interatomic distances found in **XV** are in the range of those found in the C₂B₁₀ metallacarboranes^{34,35} and other carborane molecules.³⁶

The two "carbons adjacent" isomers **XI** and **XII**, as well as their C_{cage}–H model compounds (**XI'** and **XII'**), have cage structures that are essentially the same as those of (CH₃)₄C₄B₈H₈ (isomer GA)⁴ and (C₂H₅)₄C₄B₈H₈ (isomer GB),⁵ respectively, reported by Grimes and co-workers. The defining feature of all these structures is that the cage carbons are localized on the same side of

the cluster. In **XI** and GA, the four carbons are bonded contiguously in roughly a "Z"-shaped configuration (see Figure 3). The atom-numbering system for compound **XI** used in Figure 3 requires some explanation. X-ray analysis shows a disordering of the two middle cage carbons, C(2) and C(3a), plus their bound *n*-Bu groups; the positions shown in Figure 3 are for 50% occupancy; equivalent sites across a mirror plane defined by atoms C(1), C(4), B(7), and B(9) also show 50% occupancy by a set of atoms C(2a) and C(3), plus their attendant substituents. The atoms selected to be included in Figure 3 are those that give normal bond lengths and bond angles. As shown, the molecule has a C₄B₈ cage with a C₂ axis bisecting the midpoints of the C(2)–C(3a) and the B(8)–B(8a) bonds. The average C_{cage}–C_{cage} bond distance in **XI** is 1.512 ± 0.003 Å, and no variation in the three C–C bonds is apparent. However, both the model compound (**XI'**) and isomer GA show slightly longer middle carbon bond distances (in **XI'** and GA the C(1,4)–C(2,3a) distances are 1.483 and 1.46 Å, respectively, compared to 1.511 and 1.53 Å for the C(2)–C(3a) distances). The C(1)–C(2)–C(3a) bond angle in **XI** is 107.9(4)°, which is similar to the value of 109.4(8)° reported for GA.⁴ In **XII** and isomer GB the carbon faces open up, with the distances between the two middle carbons being ~2.9 Å, so that very little interaction between these two atoms would be expected (see Table 4 and ref 5). The steric effects exerted by the cage carbon substituents are difficult to assess. The distance between the two middle cage carbons in **XI**, which contains *n*-Bu substituents, is 1.508 Å (see Table 4), which is slightly less than the 1.53 Å reported by Grimes for isomer GA,⁴ which possesses smaller CH₃ substituents. Therefore, at least for these two compounds, there seems to be little steric effect. However, if the substituents are changed to SiMe₃, *t*-C₄H₉, or PhCH₂, a substantial effect is found in that with the latter substituent, only an open isomer, equivalent to GB,⁶ was found, while the only fusion products formed with the first two substituents were the "carbons apart" compounds **III**, **IV**, and **VIII**. Figure 3 shows that the tailing C₃H₅ parts of the *n*-butyl groups are oriented on opposite sides of the compound so that the primary steric interactions are between the methylene carbons directly bonded to the cage. Increasing the steric bulk around the atoms immediately bound to the cage carbons, such as by using SiMe₃, *t*-C₄H₉, or PhCH₂ substituents, prevents the formation of the structures such as **XI**. Irrespective of the method of preparation, the presence of four trimethylsilyl substituents results only in the "carbons apart" isomers **III** and **IV**,¹⁰ while a mixed trimethylsilyl/*tert*-butyl substitution can give rise to a carborane with a cage structure of **IV**. In addition to steric effects, another factor that must be considered is the inherent stability of the different cage-carbon arrangements. The relative energies of the model compounds **III'**, **IV'**, **XI'**, and **XII'** calculated at the B3LYP/6-31G* level of theory, in kJ/mol, are 118.1, 0.0, 90.1, and 101.0, respectively. Although these values must be viewed with some caution, their relative order agrees with experiment. Of the two "carbons apart" isomers, **IV** is by far the most stable; at best, compound **III** seems to be a kinetically trapped high-energy intermediate that may be the initially formed fusion

(34) For examples see: (a) Lo, F. Y.; Strouse, C. E.; Callahan, K. P.; Knobler, C. B.; Hawthorne, M. F. *J. Am. Chem. Soc.* **1975**, *97*, 428. (b) Khattar, R.; Knobler, C. B.; Johnson, S. E.; Hawthorne, M. F. *Inorg. Chem.* **1991**, *30*, 1972. (c) Khattar, R.; Manning, M. J.; Knobler, C. B.; Johnson, S. E.; Hawthorne, M. F. *Inorg. Chem.* **1992**, *31*, 268.

(35) (a) Carr, N.; Fernandez, J. R.; Stone, F. G. A. *Organometallics* **1991**, *10*, 2718. (b) Grimes, R. N. In *Comprehensive Organometallic Chemistry II*; Abel, E. W.; Stone, F. G. A., Wilkinson, G., Eds.; Elsevier: New York, 1995; Vol. 1, Chapter 9, and references therein.

(36) Baudet, R. A. In *Advances in Boron and the Boranes*; Liebman, J. F., Greenberg, A., Williams, R. E., Eds.; VCH: New York, 1988.

product but rearranges thermally to **IV**. There is no experimental evidence for measurable amounts of the two isomers coexisting in equilibrium; once an isomer with a **IV**-like structure forms (**IV**, **VII**, **VIII**, and **XIV**), the cuboctahedron-based isomer cannot be generated from it. On the other hand, the energies of **XI'** and **XII'** are close enough so that equilibrium mixtures could exist. Grimes and co-workers reported the experimental values of the ΔH s for the conversion of several $(R)_4C_4B_8H_8$ molecules from a GA (**XI**-like) to a GB (**XII**-like) geometry, to be in the range of 6.2 kJ/mol ($R = CH_3$) to 9.8 kJ/mol ($R = C_2H_5$);⁵ these are quite close to our calculated energy difference of 11 kJ/mol for **XI'** to **XII'**.

Spectra. All compounds were characterized by their 1H , ^{11}B , and ^{13}C NMR spectra, which are summarized in Table 1. In addition, compounds **I–XIV** were characterized by IR spectroscopy (see Table 2). The IR spectra are consistent with the formulations of the compounds but offer little insight into their structures; they are presented to aid qualitative identification.

The ^{11}B NMR spectra of the *nido*-carboranes **I** and **II** are similar to those of the other *nido*-2-(SiMe₃)-3-(R)-2,3-C₂B₄H₆ carboranes^{7,13} in that all show high-field resonances in the range δ -48 to -52 ppm, due to the apical borons, with the less shielded facial borons having resonances that are shifted downfield by ~50 ppm. While the three facial borons are not equivalent, at least in the neutral compounds their chemical shifts are very similar^{22a} and often cannot be resolved; this gives rise to ^{11}B NMR spectra of two peaks with 3:1 peak area ratios as found in **II** (see Table 1).^{13a} In the same way, the spectra of the *closo*-carboranes **V**, **VI**, **IX**, and **X** are similar to those reported for their respective bis(trimethylsilyl)-substituted analogues. Both of the *closo*-1,6-C₂B₄ carboranes (**IX** and **X**) have single boron resonances at δ -14.60 and -14.94 ppm, respectively, which are close to the value of -13.9 ppm reported for *closo*-1,6-(CSiMe₃)₂B₄H₄.⁸ The effects exerted by the different cage carbon substituents are seen more in the spectra of **V** and **VI**, which show three resonances (δ 7.08, -3.14, and -12.02 ppm for **V** or δ 8.21, -2.50, and -11.99 ppm for **VI**) with 1:1:2 peak area ratios, as opposed to the two-resonance spectra found for the symmetrically substituted *closo*-1,2-(RC)₂B₄H₄ cages ($R = SiMe_3$, δ 8.4 and -11.6; $R = H$, δ 1.6 and -16.3 ppm).^{8,37} A comparison of the ^{11}B NMR spectra of **V** and **VI** with that of *closo*-1,2-(CSiMe₃)₂B₄H₄ suggests that their respective peaks at δ 7.08 and 8.21 ppm are due to the basal borons that are adjacent to the cage carbons having the SiMe₃ substituents. The assignment of the cage carbon resonances, as functions of their substituent, is uncertain. Since the ^{13}C NMR resonance in *closo*-1,6-(CSiMe₃)₂B₄H₄ is at δ 109.0 ppm,⁸ the two downfield resonances at δ 110.0 and 121.8 ppm listed in Table 1 for **IX** and **X** (the 1,6-*closo*-carboranes in this study) were assigned to the SiMe₃-bound cage carbons, with the butyl-substituted cage carbon resonances being those whose δ 's are 81.29 and 32.86 ppm, respectively. If the same relative order is assumed for all the (C₄H₉)/(SiMe₃)-bisubstituted compounds, the assignments listed in Table 1 result. However, there is no guarantee that this is correct; ab initio GIAO ^{13}C

Table 6. Calculated Energies and ^{11}B NMR Chemical Shifts (δ) for Model Compounds **III'**, **IV'**, **XI'**, **XII'**, and **XV'** ^{a,b}

Compound III'
energy -358.493 56 au
B(2), -53.46(1); B(3), -15.57(1)
Compound IV'
energy -358.538 53 au
B(3,6), -28.16; B(2), -14.96(1); B(7,8), -16.16(2); B(4,5), -5.45(2); B(1), 57.67(1)
Compound XI'
energy -358.504 21 au
B(6,5a), -32.23(2); B(8,8a), -28.10(2); B(5,6a), 14.24(2); B(7,9), 15.23(2)
Compound XII'
energy -358.500 054 au
B(5), -10.66(1); B(8), -10.60(1); B(7), -6.15(1); B(10), -6.06(1); B(9), -4.10(1); B(6), -4.06(1); B(12), 3.57(1); B(11), 3.60(1)
Compound XV'
B(16,16a), -26.47(2); B(15,15a), -15.10(2); B(7), -12.87(1); B(12,12a), -7.18(2); B(4), 61.60(1)

^a Energies of the B3LYP/6-31G*-optimized geometries. ^b δ from GIAO B3LYP/6-311G**/B3LYP/6-31G*.

NMR chemical shift calculations on *nido*-2-(SiMe₃)-3-(CH₃)-2,3-C₂B₄H₆ indicate that the SiMe₃-bound carbon may be the more shielded one.^{22a} It should be emphasized that no structural conclusions result from the relative order of the chemical shifts of the differently substituted cage carbons listed in Table 1. Therefore, while the structures of **I**, **II**, **V**, **VI**, **IX**, and **X** have not been determined by X-ray crystallography, their ^{11}B NMR spectra, as well as their methods of preparation, leave little doubt that the structures assigned to these compounds in the Experimental Section are correct. However, a direct interpretation of the NMR spectra of the fusion products **III**, **IV**, **XI**, **XII**, **XIV**, and **XV** in terms of their solid-state structures is not possible. Even though the ^{11}B NMR spectra of the three structurally characterized "carbons apart" isomers **III**, **IV**, and **XV** consist of single boron resonances at δ -30.18, -5.57, and -7.76 ppm, respectively (see Table 1), their X-ray structures show nonequivalent borons. The solid-state structure of **III** shows a C₄B₈ cage with *D*_{2h} symmetry having two sets of boron atoms (B(3,4,3a,4a) and B(2,5,2a,5a)) (see Figure 1), while, at best, **IV** and **XV** have cages with *C*_s symmetry containing five sets of borons (in Figure 5; B(4), B(17), B(12,12a), B(15,15a), and B(16,16a)). The single ^{11}B NMR resonances found for these compounds indicate fluxionality in all the "carbons apart" C₄B₈ molecules. Table 6 lists the GIAO-calculated ^{11}B NMR chemical shifts of the model compounds **III'**, **IV'**, and **XV'**; such calculations have proved useful in rationalizing the NMR spectra of a number of trimethylsilyl-substituted carboranes and metallocarboranes.²² The calculations show the expected two-peak and five-peak patterns for **III'** and **IV'**, respectively. However, rapid mixing of the boron atoms would result in single resonances at δ -35.5 ppm for **III'** and δ -7.10 ppm for **IV'**, which are close to the experimental chemical shifts of δ -30.18 and -5.57 ppm for **III** and **IV**, respectively. Figure 6 shows possible transition states for the fluxionality of each isomer; **TSIII** lies 38.34 kJ/mol higher than **III'**, and **TSIV** is 44.82 kJ/mol higher in energy than **IV'**. While these transition states are reasonable, they are not the results of an

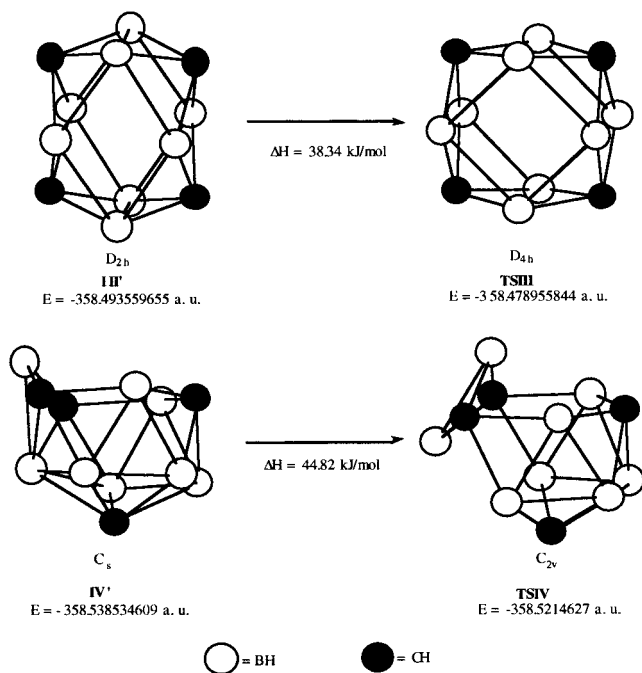


Figure 6. Possible transition states for the intermolecular rearrangements of **III'** and **IV'**.

exhaustive exploration of the different possible isomerization mechanisms. However, irrespective of the exact rearrangement mechanism, the calculations show that the experimental ^{11}B NMR spectra of **III** and **IV** are consistent with the structures given in Figures 1 and 2, respectively. This agreement also leads us to conclude that **VII**, **VIII**, and **XIV** have structures similar to that of **IV**. The observation of a single peak in the ^{13}C NMR spectrum of **IV** also indicates fluxionality, as do the spectra of **VII**, **VIII**, **XIV**, and **XV**, which show two cage-carbon resonances, one for the SiMe_3 bonded carbon and another due to carbon having the alkyl substituent. It is of interest to note that even though compound **XV** has a Br substituent on one of the boron atoms, B(14) in Figure 5, the ^{11}B NMR spectrum of the compound still shows only a single broad resonance at $\delta -7.76$ ppm, which is in the same region as that found for **IV** ($\delta -5.57$ ppm) (see Table 1), indicating that introduction of a Br substituent does not promote stereochemical rigidity. Therefore, the assumption of fluxionality of the cages shown in Figures 1, 2, and 5 can adequately account for the solution NMR of the "carbons apart" C_4B_8 fusion products.

While the solution NMR spectra of compounds **III**, **IV**, **VII**, **VIII**, **XIV**, and **XV** can be rationalized in terms of their structures, the same cannot be said for the "carbons adjacent" compounds **XI**, **XII**, and **XIII**. The ^{11}B NMR spectra of these compounds all show six resonances, but at different chemical shifts and relative intensities; in **XI** the peaks are at δ 10.42, 3.67, 1.03, -7.49 , -27.17 , and -30.49 ppm with relative peak area ratios of 2:1:1:1:2:1, and in **XII** they occur at δ 14.28, 6.33, -0.23 , -2.09 , -21.89 , and -25.45 ppm with peak area ratios of 1:2:2:1:1:1, while in **XIII** the chemical shifts are at δ 7.93, 2.12, 4.79, -5.89 , -22.46 , and -35.02 ppm with relative peak areas of 1:1:2:2:1:1 (see Table 1). The solid-state structures of **XI** and **XII**, given in Figures 3 and 4, respectively, show more symmetric cages than would be expected from their solution

spectra. While the solid-state structures of **XI** and **XII** are quite similar to those of the isomers GA and GB of the $(\text{CH}_3)_4\text{C}_4\text{B}_8\text{H}_8$ fusion product reported by Grimes,^{4,5} their solution ^{11}B NMR spectra are quite different. Grimes reported a four-resonance spectrum of relative peak areas of 1:1:1:1 at δ 10.6, 8.7, -22.3 , and -29.0 ppm for GA, whose cage structure is essentially that of **XI**, while GB, whose structure is similar to **XII**, produced a three-resonance spectrum with chemical shifts of $\delta -1.5$, -2.3 , and -10.7 ppm, with relative peak areas of 1:2:1.⁵ Several other $(\text{R})_4\text{C}_4\text{B}_8\text{H}_8$ compounds with $\text{R} = \text{C}_2\text{H}_5$, C_3H_7 all gave solution NMR spectra that were very similar to those found for $\text{R} = \text{CH}_3$.⁵ The GIAO-calculated ^{11}B NMR chemical shifts for the model compounds **XI'** and **XII'**, listed in Table 6, show patterns more similar to those of Grimes compounds than to those of **XI** and **XII**. The calculated spectrum of **XI'** is a 1:1:1:1 pattern with δ 's of 15.23, 14.24, -28.10 , and -32.23 ppm, while **XII'** would give four sets of closely spaced doublets at δ 3.60 and 3.57, -4.06 and -4.10 , -6.06 and -6.15 , and -10.60 and -10.66 ppm (see Table 6). In an effort to further establish the validity of the calculated results, the GIAO-B3LYP/6-311G**//B3LYP/6-31G* chemical shifts were calculated for $(\text{CH}_3)_4\text{C}_4\text{B}_8\text{H}_8$ with structures similar to Grimes isomers GA and GB. The calculated chemical shifts for GA are δ 15.76, 15.94, -24.55 , and -27.49 , with relative peak area ratios of 1:1:1:1; GB was calculated to be a set of four closely spaced doublets at $\delta -1.38$ (B(11)) and -1.41 (B(12)), -1.46 (B(10)) and -1.63 (B(7)), -2.54 (B(6)) and -2.66 (B(9)), and -11.96 (B(8)) and -12.03 (B(5)) ppm (the cage atom numbering system is that in Figure 4). Grimes found evidence that an additional fluxionality exists in GB that effectively rendered all four cage carbons equivalent on the NMR time scale;^{2b,5} using the cage numbering system in Figure 4, this would involve breaking the C(1)–C(2) and C(3)–C(4) bonds and replacing them by C(1)–C(4) and C(2)–C(3) bonds, which would equilibrate B(9) and B(7), B(6) and B(10), and B(11) and B(12), while B(5) and B(8) are already equivalent. The resulting ^{11}B NMR spectrum would be essentially a three-peak pattern at $\delta -1.39$, -2.07 , and -12.00 ppm with a 1:2:1 peak area ratio, which agrees quite well with the experimental 1:2:1 pattern with δ 's of -1.5 , -2.3 , and -10.7 ppm.⁵ Therefore, while GIAO can reconcile the ^{11}B NMR spectra of the $(\text{R})_4\text{C}_4\text{B}_8\text{H}_8$ carboranes (GA and GB) with their structures, similar calculations fail for the mixed alkyl-substituted carboranes **XI**–**XIII**. The spectra of all three compounds show two resonances having δ 's in the -20 to -35 ppm range, similar to that found for **XI'** and GA, but there is no agreement in the rest of the spectra. Instead of two downfield resonances, **XI**–**XIII** each have four, but with different peak area ratio patterns, which at present cannot be rationalized by reference to either the model compounds or Grimes compounds. From what is found for the other C_4B_8 compounds, these molecules probably undergo internal rearrangements and the experimental spectra are those of mixtures of isomers. For example, in the solid-state structure of **XI**, shown in Figure 1, the two *n*-Bu-substituted cage carbons are the middle ones and are directly bonded. There could be isomers in which one or more of the middle carbons had SiMe_3 substituents; such isomers should have different ^{11}B

NMR spectra and a mixture of such isomers would exhibit a complex ^{11}B NMR spectrum. Since Grimes found GA and GB to exist in equilibrium, isomers with structures based on **XI** could be in equilibrium with those based on **XII**, further complicating the spectra. Because of the uncertainty in interpreting the spectra of these compounds, it is not possible to assign a structure to **XIII**. Its ^{11}B NMR spectrum is quite different from that of its “carbon apart” analogue **XIV** and is more similar to that of **XI** than to **XII**, hence the “carbons adjacent” descriptor. However, there is no guarantee that it is not some other isomer altogether. For example, a local minimum was obtained by B3LYP/6-31G* that is only 27.59 kJ/mol higher in energy than is **IV'** and consists of a C–B–C–C–C–B six-membered ring situated above a B_5 ring and an apical boron. This would give a ^{11}B NMR spectra of five peaks of 2:2:2:1:1 relative peak area ratios at δ 14.72, 6.90, –13.63, –26.23, and –30.02 ppm, respectively, which is closer to the experimental spectra of **XI**–**XIII** than are those of **XI'**, **XII'**, or Grimes isomers.

Conclusions

The syntheses, structures, and spectral properties of the fusion products of $[\textit{nido-2}-(\text{SiMe}_3)\text{-3}-(\text{R})\text{-2,3-C}_2\text{B}_4\text{H}_4]^{n-}$ ($x = 4, n = 2, \text{R} = n\text{-C}_4\text{H}_9, t\text{-C}_4\text{H}_9, \text{CH}_3; x = 5, n = 1, \text{R} = n\text{-C}_4\text{H}_9$) are functions of both the nature of the R groups and the charge on the carborane. Two classes of C_4B_8 carboranes were obtained, a set of “carbons apart” isomers (**III**, **IV**, **VII**, **VIII**, **XIV**, and **XV**) in which all the cage carbons are separated by at least one boron atom, and the “carbons adjacent” compounds in which the carbons are localized on one side of the cage (**XI**–**XIII**). All of the carboranes were obtained as oxidative fusion products in the oxidation of the *nido*-carboranes by NiCl_2 . Normally, oxidation of the *nido*-carborane dianions ($x = 4, n = 2$) produced the corresponding *closo*-1-(SiMe_3)-2-(R)-1,2- $\text{C}_2\text{B}_4\text{H}_4$ compounds as well as the “carbons apart” fused C_4B_8 carborane. The “carbons adjacent” compounds were obtained when the monoanion was used ($x = 5, n = 1$) or as a minor product (12% yield) in the oxidation of $[\textit{nido-2}-(\text{SiMe}_3)\text{-3}-(\text{CH}_3)\text{-2,3-C}_2\text{B}_4\text{H}_4]^{2-}$; in the reaction with the monoanion, no *closo*-carborane was formed. The fusion reactions are thought to proceed through the formation of a full-sandwich nickelacarborane intermediate that decomposes to give Ni^0 and the C_4B_8 carborane product. It was speculated that the structure of this metallacarborane intermediate dictates the type of fusion product; if the cage carbons occupy a trans position across the metal in the metallacarborane, a “carbons apart” product with a structure similar to **III** initially forms, which

is converted to the thermodynamically more stable **IV**-like isomer during workup. On the other hand, when the cage carbons of the intermediate nickelacarborane are on the same side of the metallacarborane, “carbons adjacent” C_4B_8 fusion products similar to **XI** or **XII** are produced. Earlier work by Grimes on the oxidation of $[\text{2,3-(CH}_3)_2\text{-2,3-C}_2\text{B}_4\text{H}_4]_2\text{FeH}_2$ to give fusion products with structures similar to those of **XI** and **XII** served as precedents for these rationales.^{4,5} Of the two general structures found in the “carbons apart” carboranes, the one typified by **III** is unique in that its structure is that of a distorted cuboctahedron (see Figure 1), rather than one based on the icosahedron. Isomer **IV** has a more classical *nido* structure that can be visualized as arising by the opening of a face of an icosahedron to give a six-membered C_3B_3 open face that surmounts a B_5 ring and an apical cage carbon (see Figures 2 and 5). This structure is similar to those of the $[\textit{nido}(\text{R})_2\text{C}_2\text{B}_{10}\text{H}_{10}]^{2-}$ dianions, which have the same number of cage electron pairs as do the C_4B_8 compounds. The solution NMR spectra of the “carbons apart” compounds can be understood on the basis of fluxionality of the structures shown in Figures 1 and 2. Ab initio molecular orbital calculations on model compounds, where H's are the cage carbon substituents, were used to identify reasonable transition states for the fluxionality of these compounds (see Figure 6). However, the ^{11}B NMR spectra of the “carbons adjacent” compounds cannot be understood in terms of the solid-state structures of **XI** and **XII** or calculations using model compounds. The solid-state cage structures of **XI** and **XII** are essentially the same as those found by Grimes for the two isomers of $(\text{CH}_3)_4\text{C}_4\text{B}_8\text{H}_8$, but their ^{11}B NMR solution spectra are quite different. It seems that the presence of different substituents on the cage carbons may generate a number of isomers in solution that greatly complicate the spectral properties of these compounds. The study of the structures, properties, and reactivities of the C_4B_8 carboranes is continuing in our laboratories.

Acknowledgment. This work was supported by grants from the Robert A. Welch Foundation (Grant Nos. N-1322 and N-1016), the donors of the Petroleum Research Fund, administered by the American Chemical Society, and the National Science Foundation.

Supporting Information Available: Atomic coordinates (Table S-1), all bond lengths and bond angles (Table S-2), anisotropic displacement parameters (Table S-3), and H-atom coordinates and isotropic displacement coefficients (Table S-4) for **III**, **IV**, **XI**, **XII**, and **XV** (50 pages). Ordering information is given on any current masthead page.

OM980606K